On the performance of radiocarbon and quartz OSL dating in macrotidal estuarine environments: Four case studies from Western France

Thibaud Lortie, J.-P. Buylaert, M. Fruergaard, Bernadette Tessier, M. Mojtahid, M. Durand, R. Bourillot, F. Eynaud, N. Taratunina, Laurent Dezileau

Quaternary Geochronology 92 (2026) 101723

Contents lists available at ScienceDirect

Quaternary Geochronology

journal homepage: www.elsevier.com/locate/quageo

On the performance of radiocarbon and quartz OSL dating in macrotidal estuarine environments: Four case studies from Western France

T. Lortie [a,*], J.-P. Buylaert [b], M. Fruergaard [c], B. Tessier [a], M. Mojtahid [d], M. Durand [e], R. Bourillot [f], F. Eynaud [f], N. Taratunina [b], L. Dezileau [a]

[a] Normandie Univ, UNICAEN, UNIROUEN, CNRS, M2C, 14000, Caen, France
[b] Department of Physics, Technical University of Denmark, DTU Risø Campus, Roskilde, Denmark
[c] Department of Geosciences and Natural Resource Management, University of Copenhagen, Copenhagen, Denmark
[d] Université d'Angers, Université de Nantes, Université Le Mans, CNRS, LPG, UMR 6112, 2 Bd Lavoisier, 49045, Angers Cedex, France
[e] CEREMA (Centre d'études et d'Expertise sur les Risques, l'Environnement, la Mobilité et l'Aménagement), Direction Territoriale Ouest, Agence d'Angers, 23 Avenue de l'Amiral Chauvin, 49130, Les Ponts-de-Cé, France
[f] University of Bordeaux, CNRS, Bordeaux INP, EPOC, UMR 5805, F-33600, Pessac, France

ARTICLE INFO

Keywords:
Optically stimulated luminescence
14C
Macrotidal estuaries
Young sediments
Intertidal area
English channel
Atlantic Ocean

ABSTRACT

The study of estuarine sedimentary archives provides valuable insights into their geomorphological evolution over the past two centuries, enhancing our understanding of estuarine responses to climate change. Establishing a reliable and precise geochronological framework is therefore essential for monitoring these changes. This study evaluates the performance of quartz Single-Aliquot Regenerative (SAR) OSL and AMS ^{14}C dating in four estuaries along the western coast of France. The results are compared with cartographic data, serving as an independent age control. Of the 14 OSL dated samples, 10 yield depositional ages consistent with cartographic data, whereas the remaining 4 appear to overestimate ages by 20–100 years. In contrast, AMS ^{14}C dating reveals numerous stratigraphic inversions, with at least 12 out of the 16 measured samples overestimating the depositional age in some cases by up to 5000 years, in total disagreement with cartographic data. The discrepancy between the OSL and radiocarbon ages reflects the constant reworking of allochthonous material, to which is added the further uncertainty associated with the local reservoir age. These factors fundamentally limit the reliability of ^{14}C dating regardless of the material analyzed. By contrast, the OSL signal displays remarkable resilience, with any age overestimation linked to partial bleaching remaining minor (on the order of decades) compared with the errors affecting ^{14}C ages. This underscores the capacity of OSL dating to resolve short-term environmental changes and positions it as the most reliable tool for constructing high-resolution chronologies of the last centuries in macrotidal estuarine settings.

1. Introduction

Estuaries are complex environments with significant ecological, economic, and cultural value. Moreover, in the context of rising sea levels, they function as sediment traps, providing ideal sedimentary records for high-resolution paleoenvironmental studies (Colman et al., 2002). Regarding French estuaries, numerous studies have focused on understanding the evolution of these systems on a Holocene timescale (e.g., Anthony, 2000; Antoine et al., 2000; Delsinne, 2005; Durand et al., 2016). Others have examined seasonal to decadal variations (e.g., Nasseh et al., 1999; Pellerin Le Bas, 2018; Turki et al., 2021). However, only a few have explored the evolution of these environments on a multi-centennial scale (Fruergaard et al., 2020). This is partly due to the challenges of developing robust chronologies for these sedimentary archives over such a recent (decadal-centennial) timeframe.

Radiocarbon dating, commonly used in coastal areas for geomorphological reconstructions or paleoenvironmental studies (Das et al., 2013; Erlandson and Moss, 1999; Vartanian et al., 2013) faces certain limitations when applied to estuarine sedimentary archives from recent periods. The scarcity of datable continental material often requires to date the shells of marine and estuarine organisms (Olsen et al., 2017), which are sensitive to remobilization (Gao and Collins, 2014) and reservoir age issues (Stuiver et al., 1986; Stuiver and Braziunas, 1993; Stuiver and Polach, 2006). Several studies conducted in estuarine

* Corresponding author.
E-mail addresses: thibaud.lortie@orange.fr, thibaud.lortie@etu.unicaen.fr (T. Lortie).

https://doi.org/10.1016/j.quageo.2025.101723
Received 3 June 2025; Received in revised form 10 December 2025; Accepted 23 December 2025
Available online 27 December 2025

environments have shown that this reservoir age can vary locally by hundreds of years (Lougheed et al., 2016; Ulm, 2002), up to thousands of years in extreme cases (Gómez et al., 2008). In addition, these reservoir age offsets can occur over very short timescales, as demonstrated by Grimm et al. (2017), reporting ΔR variations of 260 years between two consecutive seasons (summer-autumn). One of the main reasons for this wide variation is the input of ^{14}C-depleted organic carbon from the continent, a phenomenon known as the dead carbon effect, hardwater effect, or old carbon effect, which results in an apparent aging of the dated organisms (Deevey et al., 1954; Godwin, 1951; Philippsen and Heinemeier, 2013).

$^{210}Pb_{ex}$ dating is one of the most used methods in lake and coastal environments and is often very reliable for dating recent sediments, generally providing uncertainties ranging from one year to a decade (Baskaran, 2012). However, it can be affected by sedimentary processes such as compaction, erosion, episodic sedimentation or bioturbation (Baskaran et al., 2014; Benninger et al., 1979; Miguel et al., 2003). Additionally, developing an age model requires comparison with an independent temporal marker (Barsanti et al., 2020), such as the identification of a ^{137}Cs peak from the 1962–1963 atmospheric deposition maximum (Ritchie and McHenry, 1990). Furthermore, this dating method is limited to a timescale of just over a century, as it relies on the decay of ^{210}Pb until all atmospheric excess $^{210}Pb_{ex}$ derived from ^{222}Rn has disintegrated (Swarzenski, 2013).

Technological and methodological advancements in the late nineties-early 21st century, most notably the introduction of the single-aliquot regenerative dose (SAR) protocol (Murray and Wintle, 2000) applied to coarse-grained quartz, has revolutionized the luminescence dating technique. Soon after its introduction, very young (decadal-centennial scale) accurate and precise SAR based quartz OSL ages for aeolian and coastal sediments were published (e.g. Ballarini et al., 2003; Fruergaard et al., 2011; Madsen et al., 2005; Madsen and Murray, 2009).

However, OSL dating in estuarine environments can sometimes be challenging, primarily due to the high turbidity that often characterizes these environments (Niu et al., 2022). This turbidity can result in partial bleaching of the grains, leading to an overestimation of the depositional age (e.g. Jain et al., 2004; Olley et al., 2004). Nevertheless, studies have demonstrated that complete bleaching in estuarine and deltaic contexts is certainly possible (e.g Chamberlain et al., 2017, Chamberlain et al., 2020; Madsen et al., 2005, 2007a, 2007b), though it may sometimes be limited to specific granulometric fractions depending on their mode of transport (bedload versus suspended transport) (Chamberlain and Wallinga, 2019; Nian et al., 2018; Wang et al., 2015). Tidal dynamics may be a key factor in achieving effective bleaching in estuarine environments, as they could enable sediment reworking and exposure to sunlight during low tide (Fruergaard et al., 2015; Mauz et al., 2010).

Many studies have demonstrated the limitations of radiocarbon dating and on the contrary the potential of OSL dating in fluvial mouth zones, but most of these works have focused on deltaic settings (e.g Chamberlain et al., 2017, 2018; Nian et al., 2018; Qiaola et al., 2022) which differ substantially from estuaries. Estuarine settings are characterized by strong tidal mixing, variable sediment sources, and significant marine reservoir effects, which create unique challenges for geochronology (e.g. Olsen et al., 2017). Very few studies applied OSL dating in estuaries (Fruergaard et al., 2020; Madsen et al., 2005, 2007b; Pannozzo et al., 2022), with only 2 focused on macrotidal estuaries. With respect to our regional sites, OSL dating was applied to fluvial sediments in the Loire River (Colls, 1999; Colls et al., 2001; Singarayer et al., 2005; Stokes et al., 2001; Straffin et al., 1999; Straffin and Blum, 2001; Wallinga, 2002), in the Garonne River, one of the two tributaries of the Gironde estuary (Bertran et al., 2025; Lescure, 2015), and in the Somme River (Antoine et al., 2023). Our study provides one of the few systematic, multi-site assessments of OSL and AMS ^{14}C performance specifically on young sediments in macrotidal estuaries, filling an important gap in the literature. This was achieved by applying standard multi-grain quartz OSL, in combination with the interquartile range (IQR) rejection criterion (Tukey, 1977), to date late Holocene sediments from cores collected in four macrotidal estuaries along the west coast of France The completeness of bleaching is first assessed internally by comparison with feldspar ages based on the less bleachable infrared stimulated luminescence (IRSL) and post-IR IRSL signals (e.g. Murray et al., 2012). Then, the OSL ages are evaluated alongside ^{14}C dating, cartographic information and the potential degree of insufficient bleaching is discussed. Beyond methodological comparison, the ultimate aim is to investigate the geomorphological evolution of these estuaries since the end of the Little Ice Age, approximately 200 years ago (TRESSE project: TRAjectories, EStuaries, Sediments).

2. Regional settings

Sediment cores were collected from four estuaries along the west coast of France (Fig. 1A). The Somme River and Orne River estuaries (Fig. 1B and C) flow into the English Channel, while the Loire river and Gironde estuaries (Fig. 1D and E) flow into the Atlantic Ocean. The water regime characteristics of the studied estuaries (summarized in Table 1) reveal substantial differences in water and sediment discharge, particularly between the northern (Somme and Orne) and southern (Loire and Gironde) estuaries. These differences stem primarily from the contrasting sizes of the four catchments and also reflect their geological settings, as the Loire and the two Gironde tributaries (Garonne and Dordogne) originate in mountainous regions (the Massif Central for the Loire and Dordogne, and the Pyrenees for the Garonne, Fig. 1A). The simplified lithological map of France indicates that the Orne, Loire, and the Gironde tributaries (Garonne and Dordogne) flow through regions of considerable geological diversity. These include magmatic and metamorphic units of the Massif Central, influencing the Dordogne and Loire, and of the Armorican Massif, affecting the Orne and Loire. Sedimentary units are also present, dominated by limestone, marl, and clay in the Loire, Dordogne, and Garonne, and by limestone in the Orne. In contrast, the Somme differs from the other rivers, as it drains exclusively through chalk formations.

The locations of the studied cores (Table S1), extracted using an "Amaury" vibracorer (de Resseguier, 1983), were determined beforehand through cartographic analysis. In the Orne and Somme estuaries, the cores were collected in 2023 from the upper intertidal zone (salt marsh). The two core sites are located in sheltered areas, protected by a sand spit in the Orne estuary and a pebble spit in the Somme estuary. For the Loire and Gironde, cores were collected from an intertidal mudflat in 2015 and on a tidal bar (Richard tidal bar, Virolle et al., 2020) within the main estuarine channel in 2016, respectively.

These four cores were collected in areas likely to preserve deposits from at least the past few centuries, while encompassing different types of depositional environments (from main-channel sediments to upper-mudflat deposits). This sampling strategy further enables the evaluation of ^{14}C and OSL dating reliability across the diversity of estuarine facies represented in the study. The four estuaries studied provide a representative range of French estuarine environments, including two examples of wave-dominated estuaries with well-established spits (Somme and Orne), one tide-dominated estuary (Loire), and one mixed tide- and wave-influenced estuary (Gironde) (e.g. Chaumillon et al., 2010).

3. Materials and methods

3.1. Luminescence dating

3.1.1. Sample preparation and equivalent dose measurements

Samples were collected from previously opened half sediment cores in France. The top 2 cm of the sediment surface was cleaned under low-intensity red lights prior to sampling to avoid artificial bleaching. Samples used for the luminescence signal measurements were approximately 10 cm in size and taken from predetermined areas of interest,

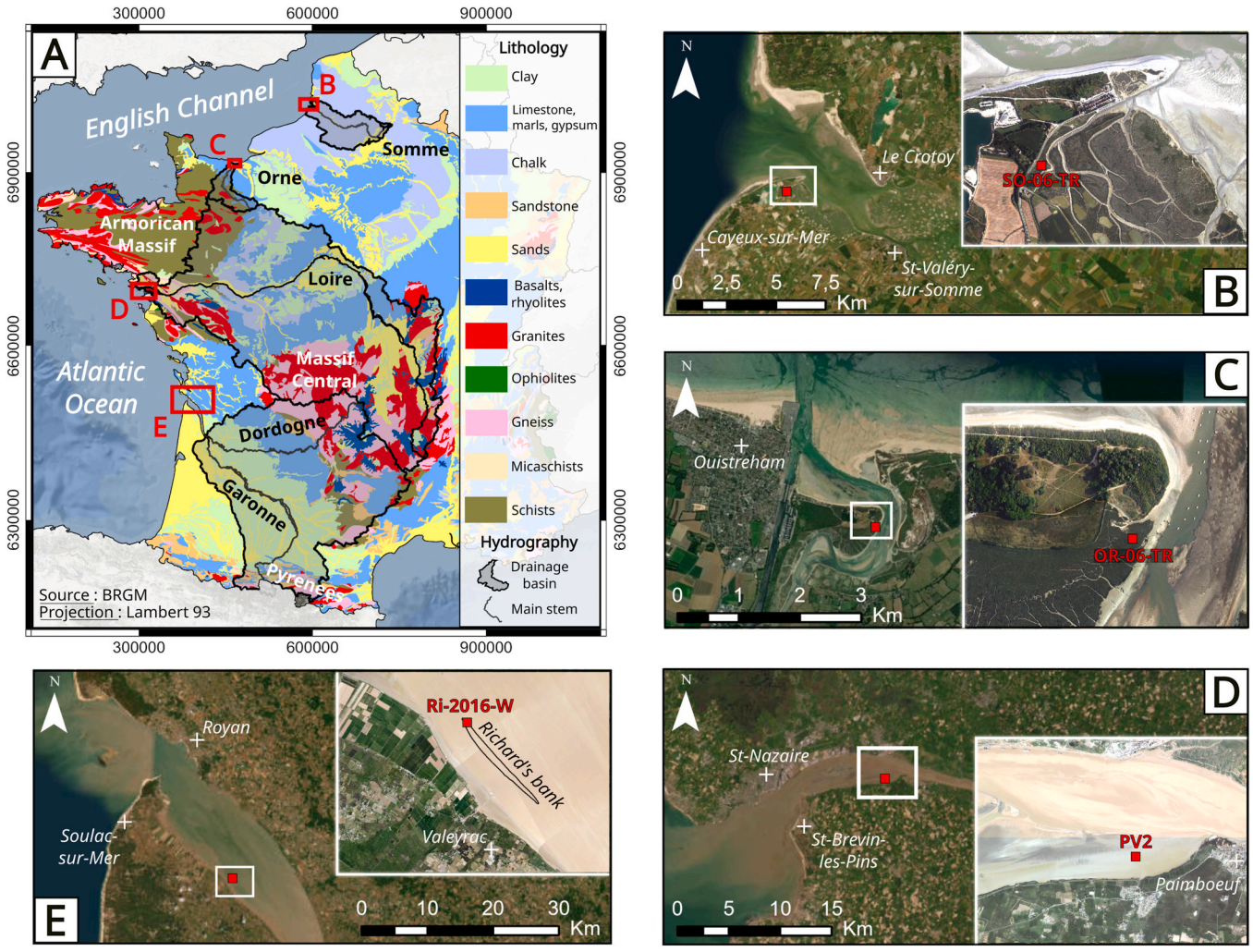

Fig. 1. A) Simplified lithological map of France showing the hydrographic features of the rivers of interest. Red rectangles indicate the locations of the estuaries shown in panels B) Somme, C) Orne, D) Loire, and E) Gironde. Red squares on the aerial photographs mark the core sampling locations. Source of aerial photographs: Earthstar Geographics. (For interpretation of the references to colour in this figure legend, the reader is referred to the Web version of this article.)

Table 1
Characteristics of the water regime of the studied estuaires. *The Gironde, being a hypersynchronous estuary, exhibits an increasing tidal range from the mouth upstream, reaching up to 6 m 130 km inland (Castaing, 1989). References: (1) SHOM, 2022; (2) Hydroportail (2023); (3) Schäfer et al. (2002); (4) Loquet et al. (2000); (5) GRESARC, 2003; (6) Figueres et al. (1985).

Estuary	Drainage basin	Tidal conditions		Fluvial water discharge		Solid sediment transport
		Mean spring tidal range (m)	Tidal gauge	Mean annual water discharges (m3/s)	Station	Mean annual sediment transport (T/Year)
Somme	English Channel	8.65 (1)	Cayeux-sur-Mer	39 (2)	Abbeville	67,800 (4)
Orne		6.60 (1)	Ouistreham	23 (2)	Thury-Harcourt-le-Hom	50,000 (5)
Loire	Atlantic Ocean	5.05 (1)	Saint-Nazaire	873 (2)	Malakoff	500,000–2,300,000 (6)
Gironde		4.20*(1)	Royan	Garonne: 649 (3) Dordogne: 448 (3)	No Data	Up to 3,240,000 (3)

with about 10 cm on each side of these zones retained for dose rate analysis. Samples were immediately packed in sealable plastic bags, stored in light-tight black bags and shipped to Denmark (DTU Risø campus).

Luminescence measurements were undertaken using both OSL on quartz and infrared stimulated luminescence (IRSL) on K-feldspar grains. Depending on the available grain-size (see Table 2), the 90–180 μm or 180–250 μm fraction were retained after wet sieving under subdued orange light (Sohbati et al., 2021), followed by treatment with 10 % HCl, 10 % H_2O_2 and 10 % HF to remove carbonate, organic matter and surface coatings, respectively (Murray et al., 2021). Owing to the limited amount of material available, 7 aliquots out of 30 from the 63–90 μm fraction were also analyzed for sample 245,508, without undergoing the 10 % HF treatment. Quartz and K-feldspar were then separated by a 2.58 g/cm^3 potassium polytungstate solution, followed by a 40 % HF bath for quartz grains, removing any remaining K-feldspar grains and etching the outer surface of quartz exposed to α-particles. Potential fluoride components were eliminated by a final treatment with

Table 2
Results of OSL and feldspar IR_{50} and $pIRIR_{150}$ analyses. Measurements were performed on the 180–250 μm fraction, except for the samples marked with an asterisk (*), which used the 90–180 μm fraction due to insufficient coarser material. For sample 245,508 (**), the 90–180 μm fraction was used except for 7 aliquots analyzed from the 63–90 μm fraction. W.C. = Water Content, na = number of accepted aliquots, nr = non-accepted aliquots.

Lab. Code	Site	Depth	W.C.	IR_{50} De	na	nr	$pIRIR_{150}$ De	na	nr	OSL De	na	nr	Feldspar dose rate	Quartz dose rate	IR_{50} age	$pIRIR_{150}$ age	OSL age	OSL age
		cm	%	Gy			Gy			Gy			Gy/ka	Gy/ka	ka	ka	ka	CE
245,501	Loire estuary	429–441	78	0.77 ± 0.02	5	1	1.53 ± 0.11	6	0	**0.63 ± 0.03**	21	2	3.59 ± 0.12	2.60 ± 0.10	0.215 ± 0.009	0.425 ± 0.033	0.244 ± 0.015	**1771 ± 15**
245,502	Loire estuary	345–357	40	1.14 ± 0.05	3	0	2.17 ± 0.12	3	0	**0.79 ± 0.04**	20	1	4.23 ± 0.16	3.24 ± 0.15	0.269 ± 0.015	0.512 ± 0.036	0.242 ± 0.018	**1773 ± 18**
245,503	Loire estuary	247–265	39	0.27 ± 0.06	6	0	1.57 ± 0.11	5	1	**0.274 ± 0.005**	21	0	4.06 ± 0.15	3.07 ± 0.14	0.065 ± 0.014	0.387 ± 0.031	0.089 ± 0.005	**1926 ± 5**
245,504*	Loire estuary	178–190	48	0.38 ± 0.02	3	0	1.49 ± 0.27	3	0	**0.251 ± 0.004**	21	0	3.94 ± 0.15	3.27 ± 0.14	0.096 ± 0.006	0.378 ± 0.070	0.077 ± 0.004	**1938 ± 4**
245,505*	Loire estuary	80–93	46	0.24 ± 0.05	6	0	1.41 ± 0.04	6	0	**0.220 ± 0.005**	20	1	4.03 ± 0.15	3.35 ± 0.14	0.060 ± 0.013	0.350 ± 0.019	0.066 ± 0.003	**1949 ± 3**
245,506	Somme estuary	198–208	36	0.31 ± 0.08	6	0	0.62 ± 0.02	6	0	**0.363 ± 0.009**	20	1	2.02 ± 0.08	1.03 ± 0.04	0.152 ± 0.040	0.309 ± 0.016	0.353 ± 0.018	**1670 ± 18**
245,507*	Somme estuary	90–103	33	0.33 ± 0.08	6	0	1.29 ± 0.15	6	0	**0.347 ± 0.007**	23	3	2.07 ± 0.08	1.39 ± 0.06	0.162 ± 0.041	0.623 ± 0.076	0.249 ± 0.013	**1774 ± 13**
245,508**	Somme estuary	2–16	54	NA	NA	NA	NA	NA	NA	**0.14 ± 0.02**	25	5	NA	1.21 ± 0.04	NA	NA	0.116 ± 0.020	**1907 ± 20**
245,509	Orne estuary	288–303	51	0.13 ± 0.02	6	0	0.343 ± 0.005	4	2	**0.105 ± 0.002**	29	4	1.72 ± 0.07	0.73 ± 0.03	0.077 ± 0.012	0.200 ± 0.010	0.144 ± 0.007	**1879 ± 7**
245,510	Orne estuary	143–162	29	0.14 ± 0.02	6	0	0.33 ± 0.02	5	1	**0.105 ± 0.003**	24	3	1.88 ± 0.08	0.89 ± 0.04	0.074 ± 0.011	0.178 ± 0.013	0.118 ± 0.007	**1905 ± 7**
245,511	Orne estuary	69–85	30	0.1632 ± 0.0010	3	0	0.31 ± 0.02	3	0	**0.102 ± 0.002**	24	3	2.00 ± 0.08	1.01 ± 0.04	0.082 ± 0.003	0.153 ± 0.012	0.101 ± 0.005	**1922 ± 5**
245,512*	Gironde estuary	576–590	59	1.56 ± 0.25	10	2	6.75 ± 0.43	7	1	**0.80 ± 0.06**	24	3	3.17 ± 0.12	2.49 ± 0.10	0.492 ± 0.082	2.129 ± 0.161	0.319 ± 0.029	**1697 ± 29**
245,513	Gironde estuary	464–484	49	1.97 ± 0.41	8	1	9.36 ± 1.02	6	2	**0.46 ± 0.05**	44	7	3.16 ± 0.11	2.17 ± 0.09	0.623 ± 0.132	2.965 ± 0.344	0.211 ± 0.024	**1805 ± 24**
245,514	Gironde estuary	62–70	44	0.94 ± 0.23	6	0	3.81 ± 0.59	5	1	**0.133 ± 0.013**	24	2	3.04 ± 0.11	2.05 ± 0.09	0.310 ± 0.078	1.254 ± 0.202	0.065 ± 0.007	**1951 ± 7**

a 10 % HCl solution.

Equivalent doses (D_e) were measured using a Risø TL/OSL DA-20 reader (Bøtter-Jensen et al., 2003) equipped with $^{90}Sr/^{90}Y$ beta sources and calibrated for coarse grains in a stainless steel cup geometry using Risø calibration quartz batch 207 (Autzen et al., 2022; Hansen et al., 2018). The SAR method (Murray and Wintle, 2000, 2003) was used for D_e estimation. Quartz luminescence was stimulated using blue LEDs (470 ± 20 nm), and the OSL signal was detected through 7.5 mm of Hoya U-340 filter. Multi-grain quartz aliquots were prepared covering the inner ~8 mm diameter of a stainless steel cup using silicone oil as an adhesive. The use of such large aliquots is common in luminescence dating of young sediments (e.g., Madsen and Murray, 2009) serves to enhance the signal-to-noise ratio, as such samples typically have low doses and sometimes weak luminescence signals.

Preheat and cut-heat settings were 160 °C for 10 s and 160 °C for 0 s, respectively, prior to a measurement under blue stimulation at 125 °C for 40 s. Aliquots were stimulated with blue light at 280 °C for 100 s at the end of each SAR cycle to ensure the removal of any residual OSL signal. An early background correction was applied (e.g. Cunningham and Wallinga (2010), subtracting from the initial signal of the decay curve (first 0.74 s) the subsequent 0.74 s of the signal as background. For each aliquot, quartz purity was checked using the OSL-IR depletion ratio (Duller, 2003), with a new 40 % HF etching for 1 h performed if this ratio was <0.90 (only necessary for sample 245,508). For age calculation of our multi-grain data we have calculated simple arithmetic means as argued by Guérin et al. (2017); extreme outliers were first removed using the interquartile range (IQR) criterion as proposed by Tukey (1977). The IQR criterion was selected over a Minimum Age Model (MAM, Galbraith, 2005) because the De distributions for the majority of samples were relatively tight and symmetric, suggesting a generally well-bleached population with a small number of outliers. The IQR provides a transparent and robust means of removing these outliers without making strong assumptions about the underlying distribution shape, which is suitable for the multi-grain approach used here.

The thermal dependence of the D_e was examined through preheat plateau and thermal transfer tests on sample 245,509, presented in section 4.2. Preheat temperatures ranging from 160 °C to 300 °C, in 20°C-increments, were applied to aliquots containing a dose of ≈0.1 Gy, with a test dose of 1.31 Gy. Thermal transfer tests were performed on the same sample by bleaching freshly made aliquots prior to measurement (two 40-s-exposures to blue light, separated by a 10,000 s pause, Madsen et al., 2007c), using the same preheat temperatures and test dose as in the preheat plateau test. Six aliquots were tested at each temperature for both experiments. Both tests showed a thermally transferred dose increase starting at ~200 °C. Based on these results, we selected a preheat temperature of 160 °C to avoid the influence of thermal transfer, as is commonly done for dating very young quartz samples (e.g. Murray and Olley, 2002; Madsen and Murray, 2009).

The suitability of the SAR protocol for our samples was assessed through dose recovery tests (Murray et al., 2021) by bleaching aliquots to release any natural trapped charge (same bleaching as in thermal transfer test). A known β-dose of 4.5 Gy was administered and then measured using the chosen SAR protocol. A total of 126 aliquots were tested, distributed across 13 samples (only sample 245,508 could not be included in this test due to the insufficient amount of quartz available).

In addition to the quartz OSL measurements, pIRIR measurements of K-rich feldspars were carried out to further investigate the quality of sediment bleaching (measurements for sample 245,508 (Somme) could not be performed due to a lack of material) (e.g. Murray et al., 2012). Given the low doses measured, it was decided to use IR_{50} and $pIRIR_{150}$ signals that do not require excessively high preheat temperatures (Madsen et al., 2011a). IRSL signals measured at higher temperatures, such as $pIRIR_{50,225}$ (Buylaert et al., 2009) or $pIRIR_{50,290}$ (Thiel et al., 2011), are often used due to their lower anomalous fading rates, but they may be affected by thermal transfer. While this effect is negligible at high doses (Murray et al., 2009), it can be problematic for young samples (Buylaert et al., 2011; Huntley and Clague, 1996). Madsen et al. (2011a) demonstrated that IR_{50} and $pIRIR_{150}$ signals can be bleached to very low levels (0.022 ± 0.002 Gy and 0.05 ± 0.01 Gy, respectively). Accordingly, our $pIRIR_{50,150}$ signal was not corrected for anomalous fading, considered negligible for such young sediments (Madsen et al., 2011a; Reimann and Tsukamoto, 2012). K-feldspar measurements were carried out using a low-temperature post-IR IRSL SAR protocol (e.g., Madsen et al., 2011a; Reimann and Tsukamoto, 2012) on 2 mm aliquots of K-rich feldspar mounted in the centre of stainless steel cups. Luminescence detection was with the blue filter package (Schott BG39 and BG3 filter combination). The IRSL signals were recorded after a 180 °C (60s) preheat, for 200s at 50 °C (IR_{50} signal) and subsequently for another 200s at and elevated temperature of 150 °C ($pIRIR_{50,150}$). Net IR_{50} and $pIRIR_{50,150}$ signals were calculated using a late background subtraction, first 2 s minus the last 20 s of the stimulation. The internal K-content of feldspar was assumed to be 12.5 ± 0.5 %, as suggested by Huntley and Baril (1997).

3.1.2. Dosimetry

Samples for dose rate measurements were dried at 105 °C for 24 h (to give 'in situ' water contents after core opening), crushed and mixed with wax to be cast in cup-shaped moulds. After a >20 days storage in this geometry to prevent disequilibrium in post-^{226}Ra series due to ^{222}Rn escape, radionuclide concentrations were measured for at least 24 h using high-resolution gamma spectrometry following Murray et al., 1987, 2018). Radionuclide activity concentrations were converted to dry-infinite-matrix beta and gamma dose rates (Table S2) using the conversion factors of Cresswell et al. (2018). Saturated water contents were measured on separate subsamples using the syringe method (Murray et al., 2021). A water content correction (Aitken, 1985) was applied by using the average of the in situ (after core opening) and saturated water content (with absolute uncertainty ±5 %); at 2 sigma this uncertainty covers the likely ranges of the burial-time average water content. An exception was made for the core from the Gironde, as it is located below the lowest astronomical tides. The saturated water content was considered the most representative. A cosmic ray contribution was incorporated based on Prescott and Hutton (1994). Total dose rates to coarse quartz and K-rich feldspar grains are presented in Table 2.

3.2. Radiocarbon dating

Radiocarbon ages were provided by accelerator mass spectrometry (AMS) performed at the Poznan Radiocarbon Laboratory in Poland (Goslar et al., 2004) and the ^{14}C measurement Laboratory in Saclay (France) through the ARTEMIS platform (Dumoulin et al., 2017; Moreau et al., 2013). For the Orne and Somme estuaries, radiocarbon dating was performed on shell samples and calibrated using OxCal 4.4.4 (Ramsey, 1995, 2009) using the MARINE20 calibration curve (Heaton et al., 2020). A weighted mean ΔR value based on the equation from Bevington and Robinson (1994) was estimated using the nearest ΔR data (i.e., ≈80 km) available on the marine reservoir correction database (Reimer and Reimer, 2001), with $\Delta R_{Somme} = -74 \pm 87$ and $\Delta R_{Orne} = -85 \pm 43$.

The ^{14}C data for the Loire (Durand, 2017; Durand et al., 2016), have been recalibrated using the IntCal20 calibration curve (the original calibration was performed with IntCal13, hence the slight difference between the data presented here and the original data). The 'Poz-85474' sample, being too recent to be calibrated with IntCal20, was calibrated using the NHZ1 post-bomb curve. The Gironde data from Virolle (2019) and Virolle et al. (2019), were also calibrated using the IntCal20 calibration curve. Table 3 presents the AMS ^{14}C dating results alongside the characteristics of the sampled material, with the shell species indicated where known.

Table 3
Properties, conventional and calibrated ^{14}C ages for the studied core. TOC = Total Organic Carbon. Unless otherwise specified, the probability of calibrated (calBP) ages is 0.95. To maximize the potential range covered by the radiocarbon ages, the calibrated (calCE) ages considered correspond to the mean of the maximum and minimum bounds at 2σ.

Lab. code	Site	Depth	Material	Conventional ^{14}C age	Calibrated age/range	Calibrated age
		cm		year BP	calBP, 2σ	calCE, 2σ
Sac-A72515	Somme estuary	124–126	Marine shell fragments (Unidentifiable)	1185 ± 30	880–485	**1268 ± 198**
Sac-A72507	Orne estuary	28–29	Marine shell fragments (Unidentifiable)	5635 ± 40	6143–5724	**−3983 ± 210**
Sac-A72508	Orne estuary	56–57	Marine shell fragments (*Cerastoderma edule*)	790 ± 30	486–160	**1627 ± 163**
Sac-A72509	Orne estuary	87–89	Marine shell (*Scrobicularia plana*)	720 ± 30	442–80	**1689 ± 181**
Sac-A72510	Orne estuary	191–192	Marine shell (*Cerastoderma edule*)	2945 ± 30	2820–2435	**−677 ± 193**
Poz-85471	Loire estuary	109–110	Plant debris	890 ± 30	831–728 (0.69) 906–864 (0.23) 858–845 (0.03)	**1133 ± 89**
Poz-85474	Loire estuary	189–190	Plant debris	126.26 ± 0.36 pMC	/	**1970 ± 12**
Poz-85475	Loire estuary	330.5–331.5	TOC	1295 ± 30	1291–1175	**717 ± 58**
Poz-85473	Loire estuary	424.5–425	Plant debris	75 ± 30	141–31 (0.69) 259–223 (0.26)	**1805 ± 114**
Poz-85477	Loire estuary	538.5–539.5	TOC	2880 ± 30	3079–2882 (0.86) 3146–3122 (0.03) 2905–2882 (0.03) 3111–3092 (0.03)	**−1064 ± 132**
2298.1.1	Gironde estuary	300	Wood fragments	273 ± 20	441–357 (0.47) 332–282 (0.43) 169–153 (0.05)	**1653 ± 144**
2275.1.1	Gironde estuary	378	Undetermined OM	2282 ± 21	2348–2304 (0.66) 2231–2180 (0.29)	**−314 ± 84**
2295.1.1	Gironde estuary	382	Wood fragments + leaves	3559 ± 22	3922–3824 (0.80) 3793–3770 (0.09) 3746–3727 (0.05) 3959–3950 (0.01)	**−1893 ± 113**
2284.1.1	Gironde estuary	415	Undetermined OM	1918 ± 21	1890–1743 (0.94) 1918–1912 (0.01)	**120 ± 88**
2293.1.1	Gironde estuary	425	Wood fragments	455 ± 25	530–481	**1445 ± 25**
2290.1.1	Gironde estuary	478	Wood fragments + seeds	102 ± 20	141–31 (0.70) 259–223 (0.25)	**1805 ± 114**
2296.1.1	Gironde estuary	589	Wood fragments + leaves	1996 ± 25	1995–1870 (0.93) 1852–1841 (0.02)	**32 ± 77**

3.3. Cartographic analyses

In this study, different sources of bathymetric data are used as independent age control. Nautical charts were used for data ranging from the early 19th century to the mid-20th century. For the Orne and the Somme, these maps also helped in selecting the coring sites, aiming to obtain records covering at least the past ~200 years. For the Somme and the Orne estuaries, the charts are military bathymetric maps produced during surveys conducted between 1816 and 1838, compiled in the "Pilote français" (Hofmann and Tesson, 2012). For the Loire, except for the 1821 chart which also comes from the Pilote Français, the surveys were conducted by the Grand Port Maritime de Resseguier (1983, 1893, 1901, 1938 and 1958).

For the Gironde estuary, the data come from bathymetric charts of the "Grand Port Maritime de Bordeaux" (1825, 1874, 1968, 1984 and 1991), with the earliest surveys dating back to 1759. For some of the above-mentioned bathymetric charts (Table S3, data type 'Points file'), survey points were already georeferenced to the lowest observed sea level by the French Hydrographic and Oceanographic Service (SHOM) and made available on their platform (https://data.shom.fr). In this case, the geodesic system was converted from WGS84 (EPSG:4326) to Lambert 93 (EPSG:2154) using ArcMap (v10.7.1). The remaining charts, not previously processed (Table S3, "Nautical charts"), were georeferenced to the Lambert 93 coordinate system. Between 10 and 30 Ground Control Points (GCPs) were employed for this purpose, using a first-order affine transformation. These GCPs are recognizable landmarks on old maps, such as lighthouses, churches, or bridges, that are still identifiable on current maps and serve as reference points. Although being a simple approach, this transformation is effective when working with a single map sheet of unknown projection and dimensions (Cajthaml, 2011). Once the georeferencing was complete, the values of the sounding points were manually marked on the maps, and, when necessary, converted from "Pieds de France" to meters (1 "Pied de France" = 0.3248 m). DEMs were created from these points using a natural neighbours interpolation method, which is often more suitable than kriging when working with datasets at irregularly spaced locations with local variations in density (Ajvazi and Kornel, 2019; Sambridge et al., 1995). The DEM derived from the 1821 point cloud of the Loire is shown in Fig. S1 for illustrative purposes. For measurements obtained by lead sounding, the vertical uncertainty is assumed to be 1 m, in accordance with SHOM guidelines and as reported in Latapy (2020), whereas bathymetric data acquired via echosounder are considered to have an uncertainty of 20 cm following Billy et al. (2012). Since the 0 m reference on historical maps is based on the lowest observed sea levels, these were assumed to correspond to the hydrographic zero (ZH) values provided by SHOM (2022).

For the post-2000 period, the analysis relied on a distinct dataset consisting of georeferenced and georectified point files derived from LiDAR surveys. These datasets were acquired as part of the National Observation Service (SNO) Dynalit for the Orne (Bretel et al., 2014; Froideval et al., 2017) and the Litto3D project for the Somme. Originally expressed relative to the "Nivellement Général de la France" of 1969 (NGF-IGN69), water depths were converted to the ZH vertical datum by adding to the initial values the difference between the chart datum and the altimetric reference (ZH/Ref in SHOM, 2022). The applied corrections amounted to +4.45 m and +4.08 m for the Somme (Touquet–Etaples station) and the Orne (Ouistreham station), respectively. Regarding the Gironde, the 2023 bathymetric data come from a digital elevation model (DEM) produced within the framework of the HOMONIM project (Paradis et al., 2024). Initially expressed relative to the level of the lowest astronomical tides, a correction of +0.46 m was applied to reference the depths to the ZH datum (Richard station).

4. Results

4.1. Sedimentary records

The Somme core (Fig. 2A) is 2.58 m long and begins with a layer of siliceous pebbles (258–220 cm) embedded in a silty matrix, followed by a fine sand facies with a silty-clay mode (220–182 cm), whose X-ray images reveal a laminated structure (alternating sandy and clayey layers) (220–182 cm). This interval is overlain by a second pebble level, followed by a sharp transition at 148 cm to much finer silty-clay facies composed of laminated sandy and clayey layers. The top 30 cm of the core are marked by significant bioturbation. The sediment record is interpreted as an intertidal flat succession with tidal rhythmites (typical sheltered estuarine facies; Tessier, 1993; 2023) aggrading behind a pebble spit. The succession ends by strongly bioturbated saltmarsh facies.

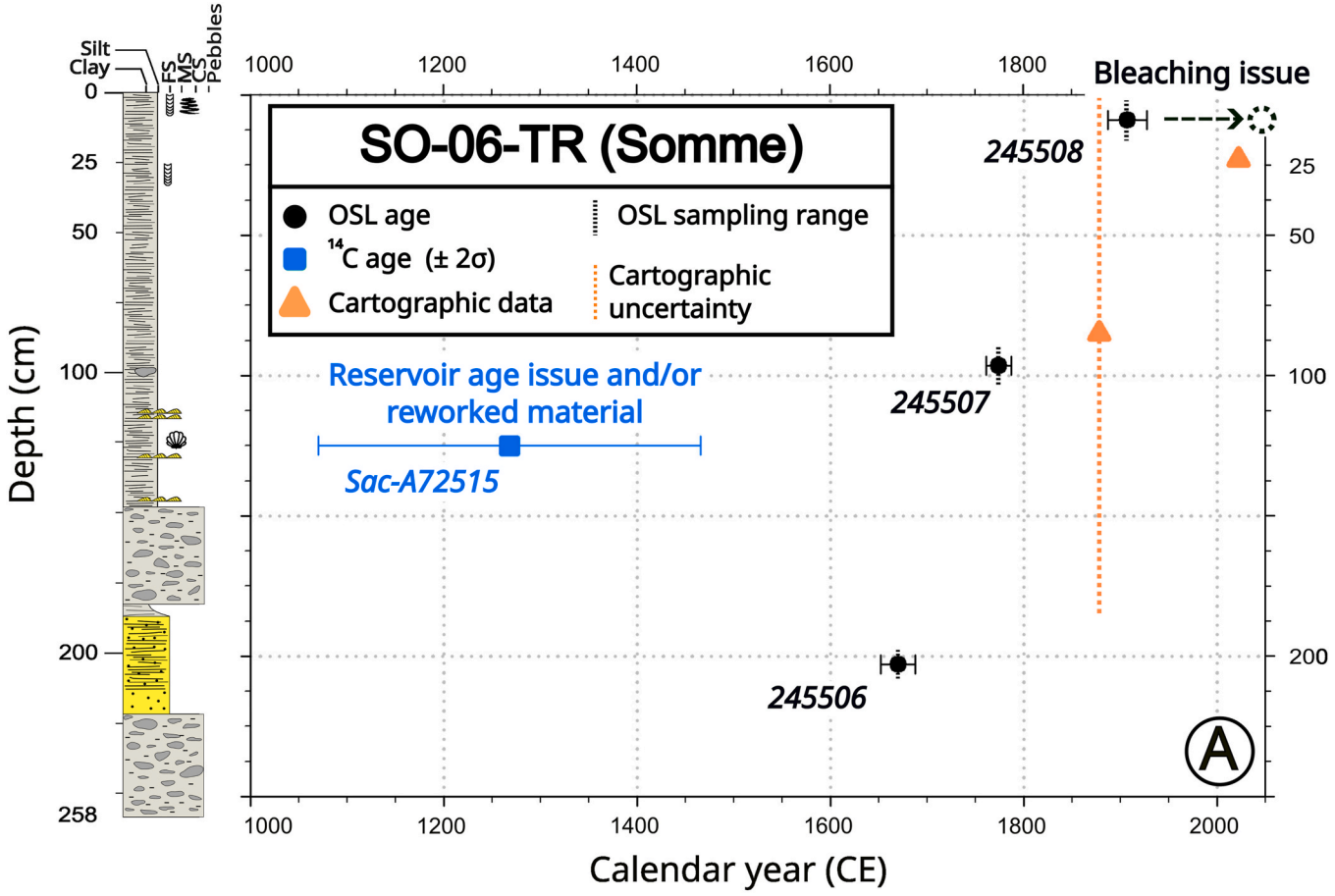

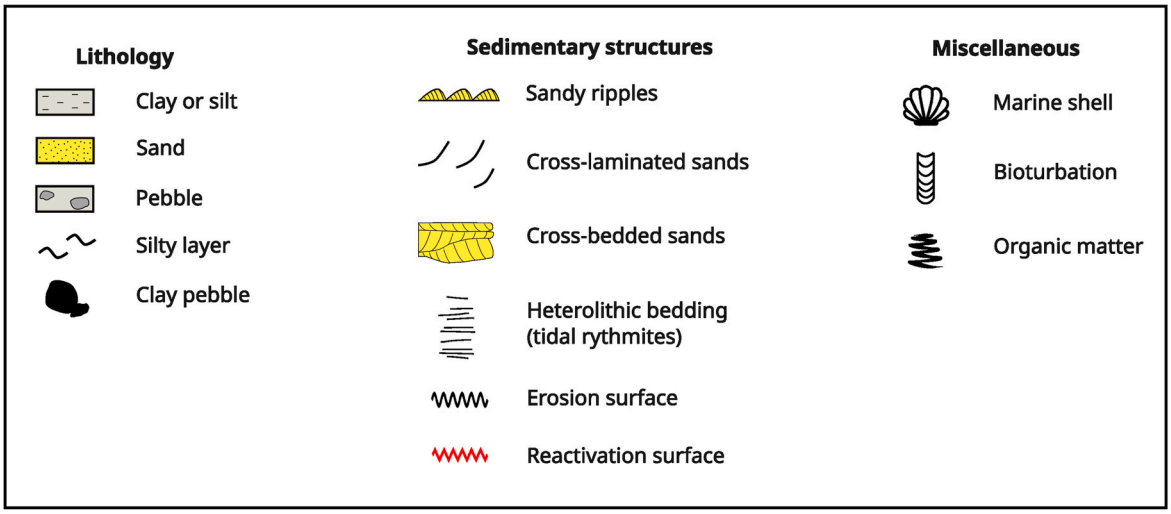

Fig. 2. Lithological logs and age-depth diagrams with chronological data and associated uncertainties from (A) Somme estuary, (B) Orne estuary, (C) Loire estuary, (D) Gironde estuary. FS = Fine sand, MS = Medium sand, CS = Coarse sand. Due to the change in scale, the uncertainties of the oldest ^{14}C dates are not directly visible in the figure but are summarized in Table 3.

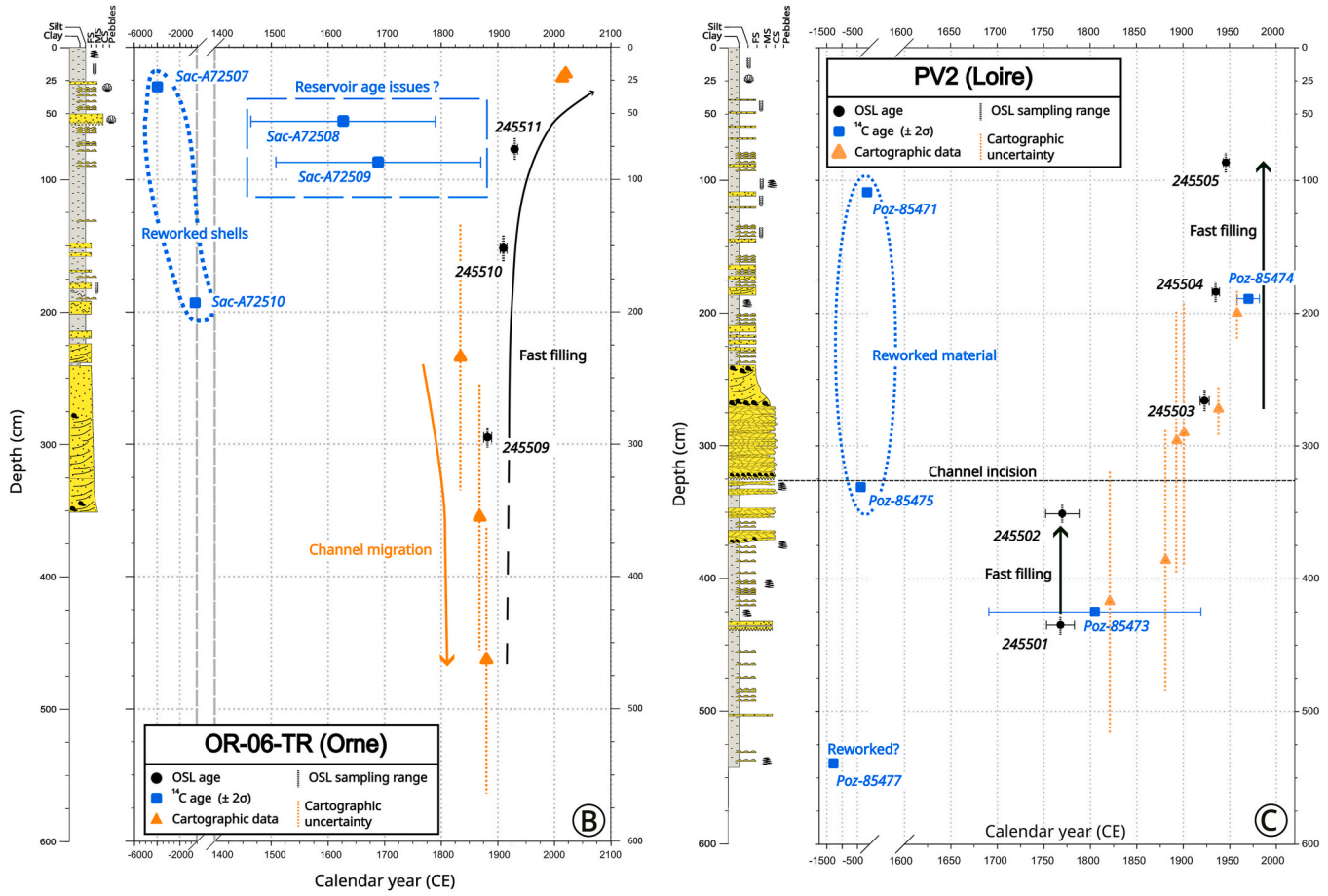

Fig. 2. (*continued*).

The Orne core (Fig. 2B) extends over 3.5 m. The lower part consists of a dark grey fine sand sequence containing clay pebbles, that gradually becomes lighter and displays unidirectional ripples (350–242 cm). The succession continues with the appearance of increasingly thick clay layers alternating with fine sand levels (242–133 cm), which eventually form a more homogeneous silty-sandy deposit (133–58 cm), occasionally interrupted by fine to medium-sized sandy beds. This sequence ends with an erosion surface at the base of a coarse sand deposit (58–50 cm). The remainder of the core is dominated by silty-clayey deposits, interspersed with sandy laminations up to 25 cm, from which bioturbation gradually increases up to the top. The succession represents a typical fining-upward sequence of tidal flat aggradation passing gradually from sandy lower flat, maybe with tidal channel facies to middle to upper flat containing heterolithic tidal facies (locally tidal rhythmites). The coarse sandy bed at the top is interpreted as a high energy layer.

The detailed description of the Loire core (Fig. 2C) can be found in Durand (2017). Measuring 540 cm in length, its lower part consists of very fine-grained deposits interspersed with fine to coarse sand beds in the lower part (540–325 cm). The succession continues with sandy deposits showing cross-stratification, followed by a coarser unit with a lag deposit at its base and cross-bedded lamination with a bidirectional pattern (325–270 cm). The sands then become finer between 270 and 230 cm, before transitioning to a heterolithic facies, shifting from wavy bedding to lenticular bedding. Bioturbation is abundant in the upper part of this section, where centimetre-wide burrows reach lengths of up to about 10 cm (230–40 cm). The last 40 cm consists of very fine deposits with abundant bioturbation. The succession is interpreted as mudflat deposits containing river flood sandy beds, incised by a tidal channel infilled by high energy tidal sand followed by a fining-upward tidal bedding succession featuring the channel abandonment.

As with the Loire core, a more detailed description of the Gironde core (Fig. 2D) can be found in Virolle et al. (2020). With a total length of 650 cm, the lower part of the core is composed of fluid mud facies associated with fine-grained sand ripples (650–543 cm). This is followed by a unit of tidal dunes made of fine to medium-grained sand with ebb-oriented foresets (543–193 cm). These dunes are regularly covered by slack water clay drapes, and include numerous clay pebbles; Reactivation surfaces are also observable within the dunes.

Organic matter-rich layers (mostly leaf debris) are also present throughout the unit. A sub-unit can be identified consisting of muddy layers characterized by thin alternations of sand ripples and amalgamated clay drapes (521–495 cm). A similar facies is observed from 193 to 158 cm, while the remainder upper part of the core (158-0 cm) consists of tidal dunes composed of fine sand with rare mud pebbles.

4.2. Luminescence results

4.2.1. Quartz OSL signal and performance tests for SAR protocol

Fig. 3A presents a sensitivity-corrected growth curve for an aliquot of representative sample 245,510. The data are well described by a single saturating exponential function, although a linear fit would also be appropriate, as the measurements lie within the low-De segment of the growth curve that could be considered as a linear region (e.g., Kitis et al., 2025). A comparison between the decay curve of this sample and that of Risø calibration quartz (Hansen et al., 2015) indicates that the signal is dominated by a strong fast component (Fig. 3B). Additionally, a comparison of the photon counts between the natural signal and a 0.5 Gy test dose confirms that the material is sensitive (Fig. 3C).

In addition to the thermal dependence of the D_e (Fig. 4A), both recycling ratios and recuperation values were documented for each

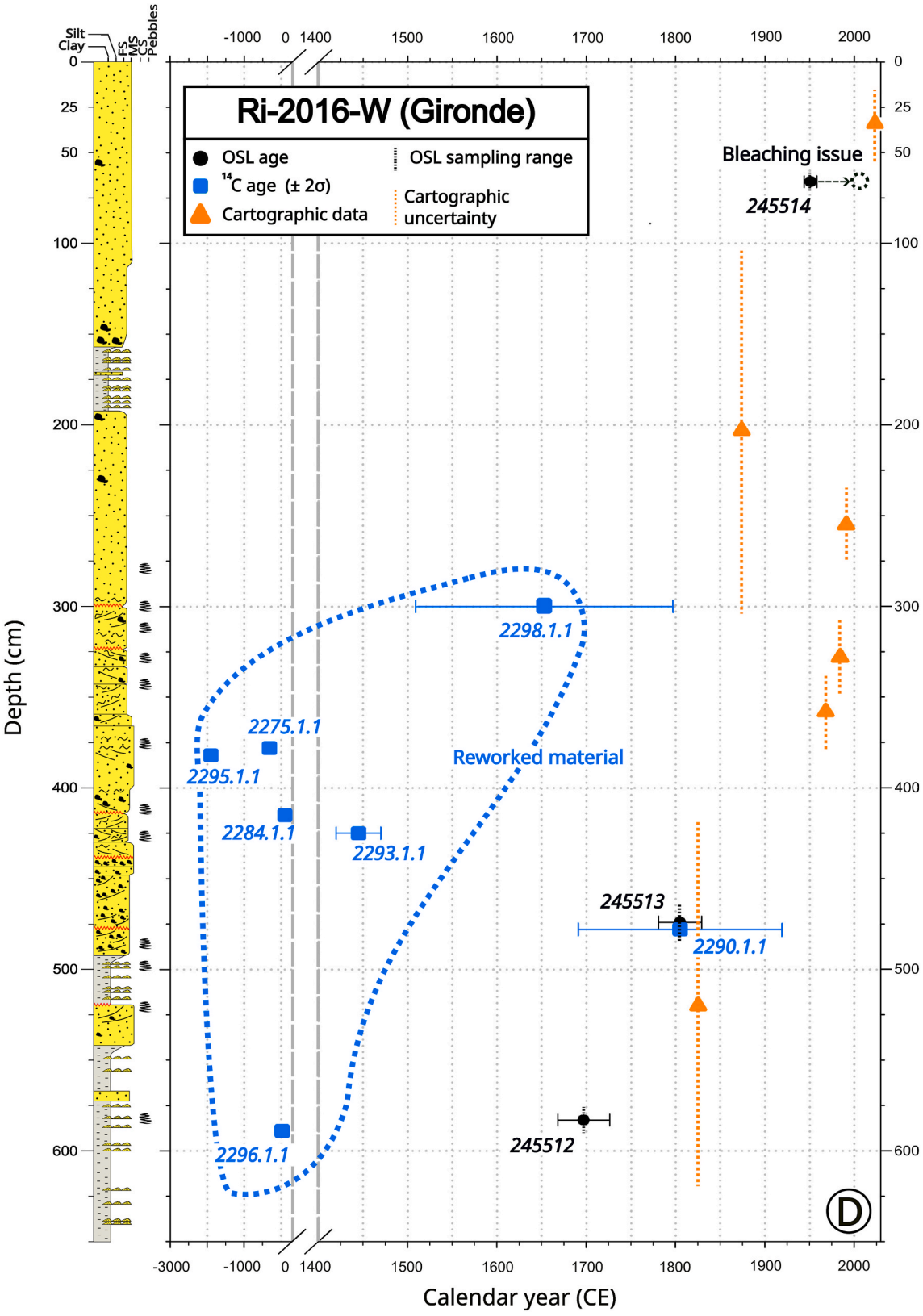

Fig. 2. (*continued*).

sample to further characterize the performance of the quartz OSL signal in our SAR protocol. As shown in Fig. 4B, the recycling ratio was satisfactory for all samples, with an average value of 0.9943 ± 0.0014 (based on 521 aliquots), demonstrating that the protocol effectively corrected for sensitivity changes. The recuperation ratio was generally below 5 % of the natural signal, with an average of 2.7 ± 0.3 % across 347 aliquots (Fig. 4C).

We conclude that our samples show excellent behaviour in a dose

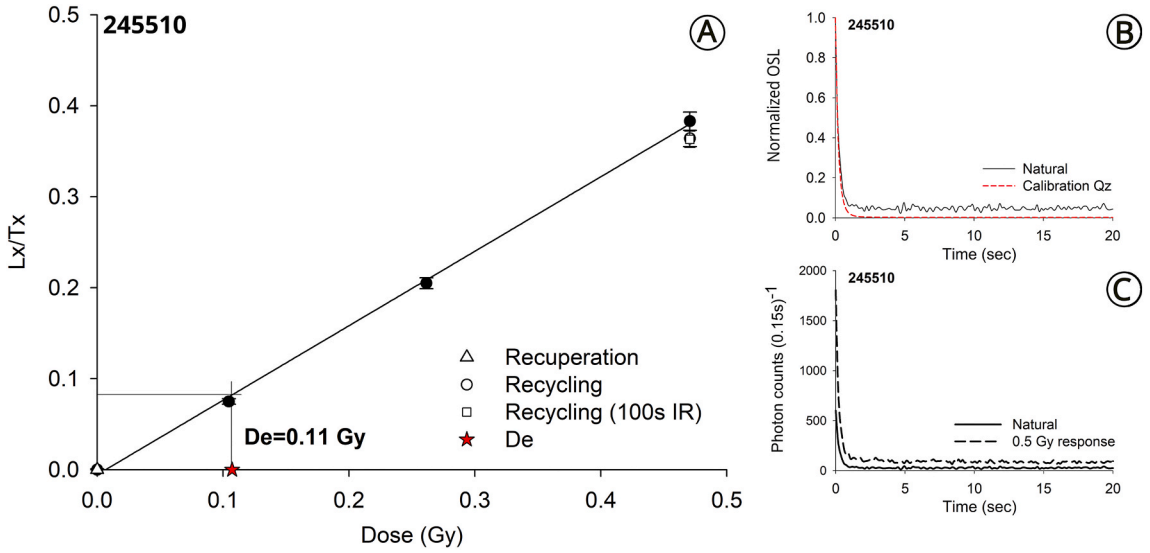

Fig. 3. A) OSL growth curve for sample 245,510. B) Normalized OSL as a function of time for the natural signal of sample 245,510 and calibration quartz. C) Photon counts values as a function of time for the natural signal of 245,510 sample and a 0.5 Gy test dose signal applied to the same sample.

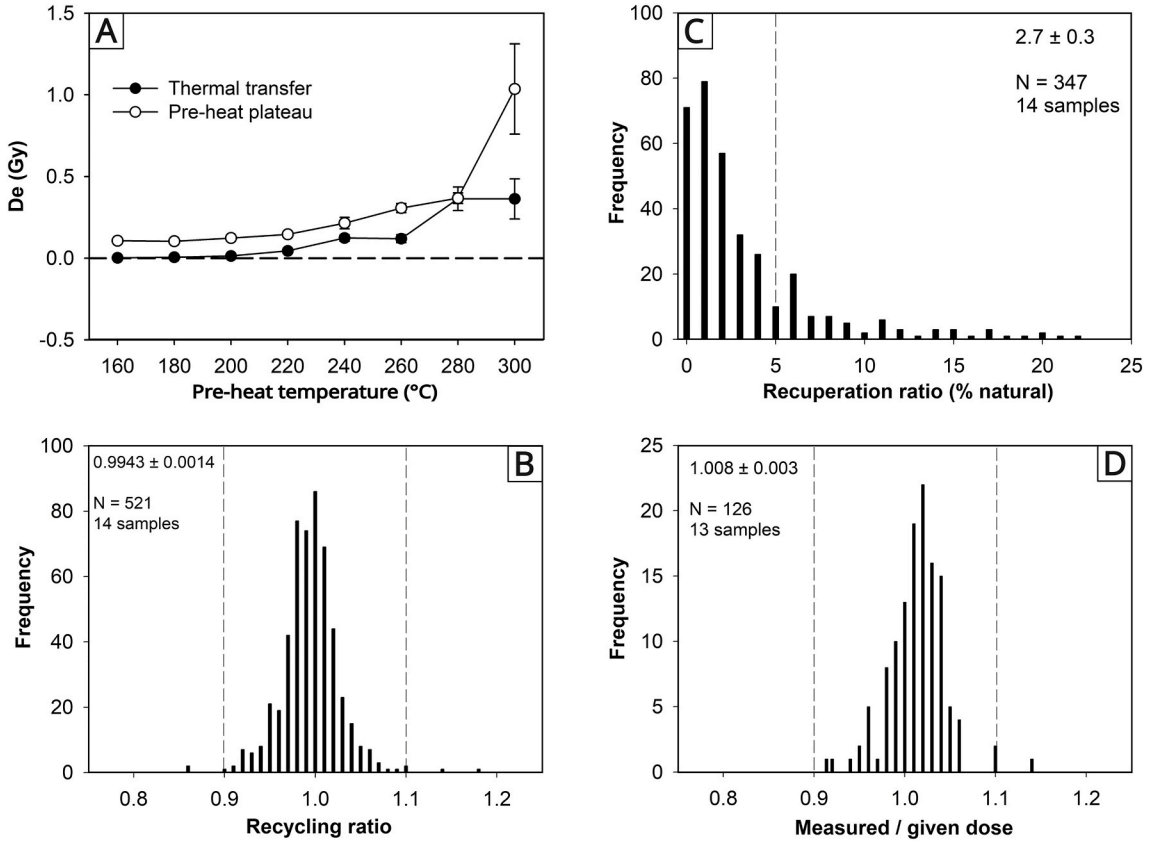

Fig. 4. Test conducted to verify the reliability of OSL measurements. A) Preheat plateau and thermal transfer tests carried out on sample 245,509. B) Recycling ratio. C) Recuperation. D) Dose recovery test (the limited amount of material available for sample 245,508 prevented it from being tested). The marked difference in the number of aliquots used for recovery and recycling tests is due to the inclusion of dose recovery tests in the recycling protocol.

recovery test with a mean measured to given dose ratio of 1.008 ± 0.003 based on 126 aliquots from 13 samples (Fig. 4D).

4.2.2. Quartz OSL ages and zeroing of the OSL signal

The D_e values, obtained by interpolating the natural sensitivity corrected luminescence signal on the growth curve, are listed in Table 2. These values are very small and range from 0.102 ± 0.002 Gy for Orne estuary to ~0.8 Gy for the Gironde and Loire estuaries. Quartz ages are also shown in Table 2 and are expressed in calendar years (CE) relative to the year of coring, i.e. 2023 for Orne and Somme, 2015 for Loire, 2016 for Gironde.

These ages are also compared with the main stratigraphic elements of the cores (Fig. 2), showing that no stratigraphic inversions are observed. All four cores are characterized by very young (decadal-

centennial scale) ages, ranging from 1670 ± 18 CE for the Somme to 1951 ± 7 CE for the Gironde. The large aliquot D_e distributions are given in Fig. S2 with accepted and rejected aliquots based on the interquartile range (IQR) criterion (Tukey, 1977); aliquots were accepted if their D_e value lay within 1.5 times the IQR. This approach has been implemented before in luminescence dating (e.g. Medialdea et al., 2014). Even though these are multi-grain aliquots which cannot fully elucidate the dose distribution within a sample, we expect that they will give some indication of the completeness of bleaching of the OSL signal; this is because typically only a few percent of the quartz grains give a luminescence signal (e.g. Duller, 2008). In addition, the applied IQR criterion will remove most of the D_e's derived from poorly bleached quartz grains. It is observed that six samples have no or only one D_e removed by the IQR criterion. Three samples (245,508, −12, −13) have quite a few aliquots with rather high D_e values that were rejected and thus appear to be poorer bleached than the other samples.

Comparison of IR_{50} and $pIRIR_{150}$ ages with OSL ages shows similar trends for the Somme, Orne and Loire estuaries (Fig. 5A–C). The IR_{50} ages generally agree with or are slightly younger than the OSL ages while the ages obtained from the $pIRIR_{150}$ signal tend to overestimate the OSL ages. In the case of the Gironde (Fig. 5D), the IR_{50} and $pIRIR_{150}$ ages significantly overestimate the quartz ages, by up to an order of magnitude for sample 245,513. These results could suggest that the quartz OSL signal may have been only partially bleached at deposition, indicating that the applied IQR criterion might not fully remove D_e values influenced by poorly bleached quartz grains. Nevertheless, it should be noted that very young quartz OSL ages were obtained for samples that have significantly larger IR_{50} and $pIRIR_{150}$ ages (e.g. Gironde sample

245,514 has a multi-grain quartz OSL age of 61 ± 7 years). In order to find out whether our quartz OSL signal is sufficiently bleached we compare our results with independent age control in the discussion.

4.3. ^{14}C dating and cartographic data

The AMS ^{14}C dating values and the nature of the sampled material are listed in Table 3, and presented alongside the cores and quartz OSL ages in Fig. 2. These values are rarely in stratigraphic order, with frequent age reversals. Furthermore, even when ^{14}C ages are internally in stratigraphic order, major discrepancies are observed between them and OSL ages, with the ^{14}C ages being significantly older. Fig. 2 also contains the age control supplied by the cartographic data; the age control points are plotted at the year of the bathymetric survey and vertical dotted lines indicate the part of the sediment column for which the cartographic age control is valid.

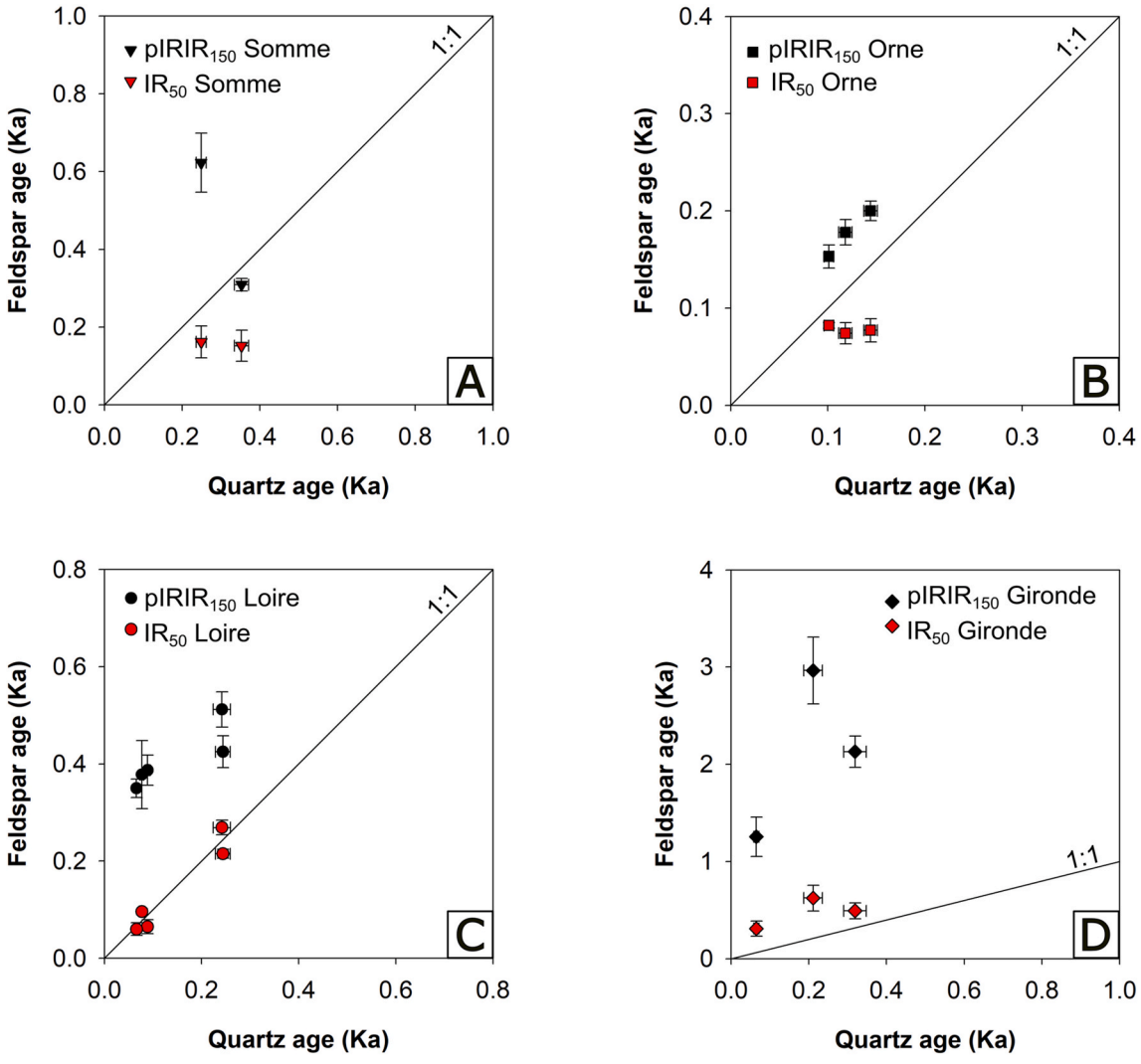

Fig. 5. IR_{50} and $pIRIR_{150}$ ages as a function of quartz OSL ages for Somme (A), Orne (B), Loire (C) and Gironde (D) estuaries.

5. Discussion

5.1. Intercomparison of the geochronological data

Our results show that the quartz from the studied estuaries is suitable for OSL dating (Figs. 3 and 4). We now compare the results of the three different chronologies (^{14}C, quartz OSL dating and cartographic age control) for each estuary individually, before drawing conclusions on the main points that emerge from this comparison.

5.1.1. Somme estuary

For the Somme estuary, the OSL ages are in stratigraphic order and consistent with the altitude of the area in 1878 CE, based on the historical bathymetric map of the area (Fig. 2A). However, the radiocarbon age of 1268 ± 198 CE is inconsistent with the abrupt facies change observed at 148 cm. The transition from a gravel facies, which is evidence of a former pebble spit hook, to a silty-clayey facies characteristic of a low-energy intertidal zone could be explained by the establishment of a new hook to the north of the area. This new hook would have protected this part of the estuary, allowing the formation of a mudflat. Dallery's (1955) work on the spit's position and evolution in 1780 CE suggests that the spit likely protected the study area between 1662 and 1783 CE, which is consistent with the OSL ages. Thus, the hypothesis of a reworked shell appears to be the most coherent, especially since the scarcity of suitable material for radiocarbon dating left us no choice but to use shell fragments. Moreover, the Somme River drains a predominantly limestone watershed (Fig. 1A), which may result in a significant input of ^{14}C-depleted dissolved carbon, thus overestimating the age of the deposits (dead carbon effect).

However, while OSL samples 245,506 and 245,507 are consistent with the map data and facies, sample 245,508 appears to overestimate the age of the surface deposits (Fig. 2A). The 2017 LiDAR survey indicates that the sediments above 25 cm of depth in the core were deposited after that date. This excludes that sedimentation had stopped or that recent deposits had been eroded, and highlights on the contrary a rapid aggradation on the site (+20 cm over six years, i.e., ~3.3 cm/year). The sampled sediments appear to be contemporary with the time of coring, indicating that the age of the deposits is overestimated by ~100 years for sample 245,508. This could suggest that sample 245,508 was not fully bleached at the time of deposition, as also suggested by the D_e distribution, and that the IQR criterion is not sufficient to remove the poorly bleached component of the D_e distribution. (Fig. S2). This overestimation could also be related to the intense bioturbation within these facies, including annelid burrows. By transporting deeper sediments toward the surface, these organisms contribute to the mixing of sediments deposited at different times, resulting in a wide range of De values (Bateman et al., 2003). This process could explain why sample 245,507, collected from the same tidal rhythmites unit but much less affected by bioturbation, does not appear to show an age overestimation and exhibits a narrower De distribution with lower overdispersion than sample 245,508 (Fig. S2).

5.1.2. Orne estuary

For the Orne estuary, analysis of historical maps reveals a period of significant erosion between 1834 and 1880 CE at the core site. During this time, the seafloor dropped from 5.14 ± 1 m to 2.57 ± 1 m CM (i.e., from 234 cm to 463 cm along the core), corresponding to an increase in core depth from 234 cm to 463 cm (Fig. 2B). This erosion results from the main tidal channel migration that was induced by the construction of dykes during the 19th century, designed to facilitate navigation in the estuary. This finding suggest that the two oldest ^{14}C samples, Sac-A72510 and Sac-A72507 at −677 ± 193 and −3983 ± 210 calCE respectively, most likely originate from reworked material.

The two remaining ^{14}C samples (Sac-A72509, Sac-A72508), dated respectively at 1689 ± 181 and 1627 ± 163 calCE, also yield ages that appear too old when compared to the cartographic data. However, it is challenging to determine whether the discrepancy stems from the remobilization of old shells and/or inaccuracies in the estimation of the reservoir age. The ages of both shells are relatively similar. While sample Sac-A72508 was collected from a sand layer interpreted as the result of a high energy event, the Sac-A72509 sample corresponds to a *Scrobicularia plana* with both valves still joined, indicating that the shell was not reworked. Taking into account the 2σ measurement uncertainty, this shell could have been deposited around 1870 CE, suggesting that a reservoir age of $\Delta R_{orne} \approx +140$ years could be more accurate. Although bivalve dating is not ideal due to their infaunal lifestyle, which can result in the burial of a contemporary organism within a much older sedimentary layer (Bouchet et al., 2009; Soares and Sobral, 2009), this cannot account for an unusually old age. Numerous studies have shown, however, that deposit-feeding bivalves, such as *Scrobicularia plana* (Hughes, 1969), can yield radiocarbon ages that are older than expected due to the incorporation of old inorganic carbon derived from calcareous sediments (e.g., England et al., 2013; Forman and Polyak, 1997; Hogg et al., 1997; Mangerud et al., 2006). Over its final 20 km, the Orne River flows through Jurassic limestone formations (Fig. 1A), making an age offset caused by the assimilation of "old" carbon a plausible explanation.

In contrast to the ^{14}C dates, OSL ages are in stratigraphic order and consistent with the cartographic data. The cross-laminated medium sand with clay pebbles appears to represent channel-filling facies which may have taken place just after the 1834–1880 CE period of erosion. This facies may indicate a very rapid channel infilling, with several meters of sediment deposited within a few years under hypertidal conditions. Considering this, along with the vertical uncertainty of old maps, even the OSL sample 245,509 does not seem inconsistent with the cartographic data from 1880 CE. Additionally, the IR_{50} ages are lower than the quartz OSL ages and the $pIRIR_{150}$ ages only overestimate by ~50 years (Fig. 5B). Thus, it appears that the OSL samples were sufficiently bleached and the IQR criterion adequately removes the few poorly bleached outliers.

5.1.3. Loire estuary

In the Loire estuary, several ^{14}C ages are also inverted within the stratigraphic column (Fig. 2C). During the initial analysis of this core, the ^{14}C samples Poz-85474 and Poz-85473 were discarded, as they were considered too young based on the extrapolation of the sedimentation rate from $^{210}Pb_{ex}$ measurements (Durand, 2017). However, OSL samples 245,501 and 245,504 support the validity of the younger ^{14}C ages while indicating that Poz-85471 and Poz-85475 are overestimating the age of sediment deposition. This is further confirmed by the cartographic data which indicates ages consistent with the most recent ^{14}C values. The excessively old ^{14}C values for Poz-85475 samples dated on bulk organic matter, suggest the potential presence of an unaccounted sediment age reservoir (Lougheed et al., 2017). This reservoir effect could arise from the erosion of old organic matter-rich soils. The Poz-85477 radiocarbon age (1064 ± 132 CE) cannot be independently verified due to the absence of supporting OSL or cartographic data. This sample, significantly older than the other, was obtained from the same fluid mud facies which appears to have been deposited quickly, as suggested by the OSL dates and the low degree of bioturbation. Despite the presence of an erosional surface at 438 cm, which prevents ruling out the hypothesis that significant erosion exhumed much older deposits, it is likely that this sample, also dated using bulk organic matter, originates from reworked material.

The OSL data are very similar to the cartographic data, except for a probable overestimation of a few decades for samples 245,504 and 245,505. These two samples appear slightly too old (by about 20–40 years) when compared to the 1958 bathymetric survey and ^{14}C dating at 190 cm. Although D_e value dispersion remains low, incomplete bleaching remains a plausible hypothesis, explaining the discrepancy between cartographic and OSL data. It could be caused by the high turbidity in the estuary (suspended solids value ranging between 1 and

2 g/L, and up to 4 g/L during flooding at Paimboeuf, according to data from the SYstème de Veille dans l'Estuaire de la Loire (2023). These two samples are also the only ones from the Loire obtained from bioturbated sediments, which may have contributed to a slight overestimation of age (Bateman et al., 2003), yet the limited spread of De values suggests that the mixing of grains from different horizons is very limited. Nevertheless, even under these theoretically unfavourable conditions for OSL dating, any overestimation of OSL ages, if present, appears to be relatively minor, even in facies associated with high-intensity events and higher turbidity. OSL samples, which have very recent ages and are closely aligned with cartographic data, suggest a modification of the age model proposed by Durand et al. (2016). Our new chronostratigraphy suggests a very rapid aggradation of the estuarine mudflats, with sedimentation rates exceeding 28 mm/year after the channel shifted at the beginning of the 20th century, as highlighted by deposits ranging from 320 to 240 cm.

5.1.4. Gironde estuary

The ^{14}C ages from the Gironde estuary exhibit variance in age distributions, with numerous inversions (Fig. 2D). Based on the cartographic data, 5 out of 7 of the ^{14}C dates appear to be anomalously old. Similar to the ^{14}C dates from the Loire, this discrepancy is likely due to the erosion of soils containing old organic matter, which is then deposited onto a more recent sedimentary layer. This phenomenon is particularly evident in the case of dates obtained from old wood or twigs, as these materials can persist on the ground for centuries without fully decomposing and are eventually being transported to the river (Barnekow et al., 1998; Wright, 2017). The sample 2296.1.1 at 589 cm cannot be directly excluded based on the cartographic data, but it is not compatible with the OSL age 245,512 (576–590 cm), which gives an age ~1700 years younger. No evidence in the core seems to indicate erosion that could explain this age offset, while sample 245,512 appears consistent with the rest of the OSL and cartographic data, suggesting that sample 2296.1.1 is reworked. Unfortunately, no cartographic data from the late 17th century with greater accuracy is available to confirm this hypothesis. Thus, only the ^{14}C age of 1805 ± 114 cal CE at 478 cm (sample 2290.1.1) appears credible given the position of the channel bottom in 1825. This dating is also consistent with the age of 1805 ± 24 CE provided by OSL sample 245,513. Cartographic data, however, suggests that sample 245,514 dated to 65 ± 7 years overestimates the age of the deposit by ~60 years. According to the 1968 bathymetric survey, deposits dating from 1951 CE should be located approximately 3 m lower, below a depth of 3,5 m.

The high D_e dispersion values and IRSL ages significantly exceeding the quartz age (up to an order of magnitude for $pIRIR_{150}$), suggest some degree of partial bleaching, equivalent to a few tens of milligray. This would explain the ~60 year overestimation for 245,514; we cannot rule out that samples 245,512 and 245,513 also overestimate the depositional age by a few decades.

The Gironde estuary is subject to a significant presence of silts and clays transported in suspension. Turbidity values frequently exceeding 1000 NTU (i.e 1 g/L, in Jalón-Rojas et al., 2015) during the winter period, as recorded by the Gironde estuary MAGEST (Marel Gironde ESTuary) survey from 2023 at Pauillac station). This high turbidity, combined with the presence of sand, promotes the formation of clay coatings around quartz grains (Dowey et al., 2012; Duteil et al., 2020, 2022; Griffiths et al., 2021; Virolle et al., 2019a, 2019b Wooldridge et al., 2017). This type of coating has been observed on sediments from our Gironde core Ri-2016-W, as well as on two other cores taken from Richard's bank as part of studies by Virolle et al. (2020). The average content of coated grains was estimated at 17 % across all the sediments from this tidal bar. The presence of clay coatings could hinder sediment bleaching, particularly for sediments eroded from the estuary banks and redeposited nearby (e.g. Stokes et al., 2001.). Although, to our knowledge, no study has quantified the impact of clay coatings on the bleaching efficiency of sediments, it can be supposed that they tend to increase the risk of partial bleaching. However, despite the presence of clay coatings of variable thickness, Perilla-Castillo et al. (2023) obtained single-grain quartz OSL ages consistent with radiocarbon dates from fluvial sediments of the Tennessee River (USA). Similarly, Jankowski et al. (2015) reported single-grain ages that appear reliable for a moderately sorted sand facies with continuous clay coatings (unit SP4) at MacCauley's Beach, New South Wales, Australia. In the case of our study, the overestimation obtained from large aliquots using the IQR criterion does not appear to exceed a few decades. Future single-grain analyses (Duller, 2008) on our known-age samples, combined with a MAM model, could help to obtain even more accurate quartz OSL ages. Additionally, single-grain dose distributions of a suite of modern analogue samples (e.g., suspended sediments) would be valuable for better constraining residual doses in tidal sediments. The strong sediment dynamics of the Gironde area, particularly of the tidal bar, as previously studied by several authors (Billy et al., 2012; Chaumillon et al., 2013; Fenies and Tastet, 1998; Froidefond and Castaing, 1978; Migniot, 1971), underscore the importance of precise stratigraphic data for understanding the evolution of these environments. Recent analyses conducted by Virolle (2019) highlight the mobility of Richard's Bank since the early 20th century, characterized by multiple phases of lateral migration, as well as alternating periods of accretion and erosion. The new stratigraphic data obtained from this core further support this strong sedimentary dynamic. This is evidenced by the high deposition rates, exceeding 20 mm/year, recorded since the appearance of Richard's Bank at 495 cm, along with the presence of erosion and reactivation surfaces that reflect the bank's erosion by tidal currents.

5.2. Reliability and limitations of the chronological data obtained

5.2.1. Reliability of ^{14}C dating

In this study, 16 radiocarbon samples were dated by AMS spectrometry, including carbonate shells, total organic carbon (TOC) and terrestrial plant debris.

Among the five shell samples, none yielded an age consistent with the OSL or cartographic results. In addition to being affected by the remobilization and transport processes that characterize all estuarine systems (e.g., Angulo et al., 2008; Colman et al., 2002), this type of material records a ^{14}C age influenced both by the marine reservoir effect and by inputs of ^{14}C-depleted organic carbon from the continent, two parameters subject to strong spatial and temporal variability (e.g., Lougheed et al., 2013). Tisnérat-Laborde et al. (2010) quantified this reservoir age across the northeastern Atlantic using bivalve and gastropod shells of known age from the collections of the National Museum of Natural History in Paris. In the central and eastern English Channel, where the Orne and Somme estuaries are located, the four tested samples show ΔR values ranging from −169 ± 56 to 15 ± 50 years. None of these samples, however, were collected near an estuary mouth, and thus they do not reflect the "dead carbon" issues encountered in estuarine settings, where ΔR values of several hundred years can occur (e.g., Holmquist et al., 2015; Ingram and Southon, 1996; Philippsen and Heinemeier, 2013). Conversely, other studies have reported low or even negative ΔR values in estuaries (e.g., Russell, 2011), which may result from the incorporation of ^{14}C in equilibrium with the atmosphere through the decomposition of terrestrial organic matter in catchments lacking carbonate bedrock (Olsen et al., 2017). Such estuarine ΔR variability highlights the need to quantify the reservoir effect locally, for example using radionuclide dating (Sabatier et al., 2010). Nevertheless, this precaution may still be insufficient, particularly for dates obtained on infaunal organisms, where ΔR variations of 100–200 years have been observed within a single shell due to seasonal and annual changes in riverine inputs (Culleton et al., 2006; Grimm et al., 2017). All these factors make this type of material virtually unsuitable for dating estuarine sediments deposited within the past several centuries.

Radiocarbon dating on bulk sediment (TOC) also presents significant

challenges in such settings: in the present study, both analyzed samples yielded ages overestimated by more than 1000 years. This reflects strong spatial and temporal variability in the carbon source pathway, including inputs of ^{14}C-depleted carbon, that can produce substantial ^{14}C age offsets (Lougheed et al., 2017). It is therefore unsurprising that the best results were obtained from dates on terrestrial plant material, with three out of eight samples yielding ages consistent with the OSL and cartographic data, and a fourth providing a plausible but unverified age. Although this type of material is likely the most suitable choice for ^{14}C dating of young sediments in macrotidal estuarine settings, it remains subject to reworking issues, particularly when dealing with material that can take several centuries to decompose (Barnekow et al., 1998).

5.2.2. Reliability of quartz OSL dating

Among the fourteen samples dated by OSL, four appear to yield ages that slightly overestimate the true depositional age, by a few decades (samples 245,504 and 245,505 from the Loire and 245,514 from the Gironde) to a maximum of 100 years (sample 245,508 from the Somme). This outcome is highly encouraging, as it indicates that the sediments provide a measurable luminescence signal despite their short burial duration, and that in most cases bleaching was sufficient to prevent any residual dose from biasing the ages (Madsen and Murray, 2009). Moreover, the measured samples exhibit a good OSL sensitivity, a critical parameter for obtaining reliable ages in young sediments (Pietsch, 2009), regardless of the estuary investigated, and thus independent of the nature of the upstream catchment. This is noteworthy given that catchment characteristics can influence OSL sensitivity, in addition to the frequency of reworking and burial cycles (Pietsch et al., 2008; Fitzsimmons, 2011). The present results therefore demonstrate that the sedimentary material from the four studied estuaries is well suited to OSL dating of young deposits.

With respect to reliability according to grain size, examination of the dated lithofacies indicates that the partially bleached samples correspond to silty–sandy facies (245,508) and fine sands (245,504, 245,505, 245,514), which account for 2 and 10 out of 14 of the samples analyzed in this study, respectively. We also obtained one well-bleached sample in the silty–sandy deposits (245,507) and seven well-bleached samples in fine sands. By contrast, samples 245,501 and 245,502 from the Loire, collected respectively from overbank flood deposits and from the base of a channel-fill sequence, exhibit a modal grain size in the coarse-sand range and show no evidence of incomplete signal resetting prior to burial. From the analysis of our case studies, we cannot conclude that grain size is a critical parameter for OSL dating.

Several studies carried out in deltaic environments, whether macrotidal or not, shown that fine (silt-rich) fractions generally provide reliable OSL ages whereas sand-sized fractions are less favorable because of incomplete bleaching and/or poorer quartz sensitivity (Nian et al., 2018a, 2018b; Wang et al., 2015; Chamberlain et al., 2017; Chamberlain and Wallinga, 2019). However, some other works have demonstrated that sand-sized fractions yield reliable ages in deltaic settings (Gao et al., 2017; Kim et al., 2015; Yi et al., 2014). In estuarine settings, Madsen et al. (2005) reported from fine-grained sediments (90–180 μm fraction extracted from a muddy matrix) very young OSL ages in the Varde River estuary (Wadden sea, from 7.0 ± 1.5 to 305 ± 16 years) in good agreement with independent ^{210}Pb and ^{137}Cs measurements. In other cores at the mouth of the Varde River estuary, Madsen et al. (2007a, 2007b) performed OSL dating on both 63–90 and 90–180 μm fractions. These ages were also found to be consistent with ^{210}Pb measurements. In the Ribble estuary (UK), Pannozzo et al. (2022) performed OSL dating on fine-grained fraction of salt marsh deposits (50–90 μm) with reliable result based on the very young age of the dated sediments (from 67 ± 9 to 264 ± 26 years). Finally, Fruergaard et al. (2020) obtained reliable OSL ages corroborated by independent radiocarbon dating, ranging from 200 ± 30 to 1050 ± 70 years in tidal-shoal facies of the Ay estuary (NW France), composed of very fine to coarse sands. These studies in estuarine settings, together with our results, demonstrate that reliable OSL dating can be obtained either in fine- or coarse-grained fractions. In deltaic settings, reliability has been found to decrease in coarse-grained sediments, with the authors suggesting that coarse sand transported as bedload may undergo incomplete bleaching due to the turbidity of the overlying water (Nian et al., 2018b). The observation that reliability appears to be high for both fine- and coarse-grained fractions in estuarine deposits remains poorly understood. We suggest that the intense sediment mixing induced by tidal dynamics could provide a plausible explanation.

Finally, three of the five samples from bioturbated layers (245,504, 245,505, and 245,508) apparently exhibits overestimated ages, suggesting that bioturbation may have offset the OSL age. It has been recognized that bioturbation may interfere with OSL chronologies (e.g., Bateman et al., 2003; 2007). In tidal-flat environments, Madsen et al. (2011b) demonstrated that *Arenicola marina*, a deposit-feeding polychaete, ingests sediment at depth and releases it at the sediment–water interface, causing OSL ages to be underestimated. The sediment brought to the surface is then highly likely to be bleached and subsequently dispersed, while the void left by the burrow is filled with surrounding younger sediments, causing the underestimation. Since overestimation of OSL ages has never, to our knowledge, been attributed to bioturbation in previous studies, the most plausible explanation remains incomplete bleaching at deposition.

6. Conclusion

In this study, we explored the potential of standard multi-grain quartz OSL and radiocarbon dating to date young deposits in macrotidal estuaries along the western coast of France, using cartographic data as independent age controls. For all samples, the quartz OSL signal is very bright and dominated by a fast component, providing stratigraphically coherent ages that align with cartographic data for 10 out of 14 samples. Incomplete bleaching of the quartz OSL can explain the overestimation observed in the four remaining samples, ranging from 20 to 40 years for two samples from the Loire Estuary, ~60 years for one sample from the Gironde Estuary, and up to ~100 years for one sample from the Somme Estuary. No modern analogues exist (sediment currently being transported in the estuary) to determine the residual quartz OSL dose offset that may influence OSL dating in these estuaries. In contrast, ^{14}C dating exhibits numerous stratigraphic inversions. According to cartographic data, only 4 out of 16 dated samples appear to yield plausible ages, whereas at least 12 show substantial overestimations of up to 5000 years. These observations relate to the strongly fluctuating hydrodynamic conditions prevailing in these macrotidal estuarine environments, which drive the continuous reworking of allochthonous material regardless of its nature, to which are added uncertainties surrounding reservoir-age estimation. These results highlight the precautions that must be applied when interpreting geochronological data in high-energy estuarine settings, and demonstrate that SAR OSL dating appears to be the only viable method for constructing high-resolution chronologies for the last centuries in such settings.

CRediT authorship contribution statement

T. Lortie: Writing – review & editing, Writing – original draft, Visualization, Validation, Supervision, Project administration, Methodology, Investigation, Formal analysis, Data curation, Conceptualization. **J.-P. Buylaert:** Writing – review & editing, Writing – original draft, Visualization, Validation, Supervision, Resources, Project administration, Methodology, Investigation, Formal analysis, Data curation. **M. Fruergaard:** Writing – review & editing, Visualization, Validation, Project administration, Methodology, Formal analysis, Data curation. **B. Tessier:** Writing – review & editing, Visualization, Validation, Supervision, Project administration, Funding acquisition, Formal analysis, Data curation, Conceptualization. **M. Mojtahid:** Writing – review & editing, Visualization, Formal analysis, Data curation. **M. Durand:**

Writing – review & editing, Visualization, Formal analysis, Data curation. **R. Bourillot:** Writing – review & editing, Visualization, Investigation, Formal analysis, Data curation. **F. Eynaud:** Writing – review & editing, Visualization, Validation, Formal analysis, Data curation. **N. Taratunina:** Writing – review & editing, Visualization, Investigation, Formal analysis, Data curation. **L. Dezileau:** Writing – review & editing, Visualization, Supervision, Funding acquisition, Formal analysis, Data curation.

Declaration of competing interest

The authors declare that they have no known competing financial interests or personal relationships that could have appeared to influence the work reported in this paper.

Acknowledgements

The present study was supported by the French Biodiversity Office (OFB, TRESSE project, grant no 21.0454). This work is part of T. Lortie's PhD thesis funded by the Normandy Region and the Regional Directorate for the Environment, Planning, and Housing (DREAL) of Normandy through the TRESSE-N project. The authors thank Vicki Hansen for her technical assistance. Emilie Jaffre is thanked for her work on the impact of the Orne coastal management during her final Master's 2 internship. Vincent Hanquiez is acknowledged for his help in acquiring some cartographic data of the Gironde.

Appendix A. Supplementary data

Supplementary data to this article can be found online at https://doi.org/10.1016/j.quageo.2025.101723.

Data availability

Data will be made available on request.

References

Aitken, M.J., 1985. Thermoluminescence Dating. Academic Press.

Ajvazi, B., Kornel, C., 2019. A comparative analysis of different DEM interpolation methods in GIS: case study of Rahovec, Kosovo. Geod. Cartogr. 45, 43–48. https://doi.org/10.3846/gac.2019.7921.

Angulo, R.J., de Souza, M.C., Assine, M.L., Pessenda, L.C.R., Disaró, S.T., 2008. Chronostratigraphy and radiocarbon age inversion in the Holocene regressive barrier of Paraná, southern Brazil. Mar. Geol. 252, 111–119. https://doi.org/10.1016/j.margeo.2008.03.006.

Anthony, E., 2000. Marine sand supply and Holocene coastal sedimentation in northern France between the Somme estuary and Belgium. Geol. Soc. Lond. Spec. Publ. 175, 87–97. https://doi.org/10.1144/GSL.SP.2000.175.01.08.

Antoine, P., Bahain, J.-J., Voinchet, P., Limondin-Lozouet, N., Auguste, P., Locht, J., Coutard, S., Dabkowski, J., Hérisson, D., Moncel, M.H., 2023. The Last 1 Ma Record from the Fluvial Terraces System of the River Somme Valley (Northern France) and the Background of the Earliest Acheulean Occupation of Northwestern Europe.

Antoine, P., Lautridou, J., Laurent, M., 2000. Long-term fluvial archives in NW France: response of the Seine and Somme rivers to tectonic movements, climatic variations and sea-level changes. Geomorphology 33, 183–207. https://doi.org/10.1016/S0169-555X(99)00122-1.

Autzen, M., Andersen, C.E., Bailey, M., Murray, A.S., 2022. Calibration quartz: an update on dose calculations for luminescence dating. Radiat. Meas. 157, 106828. https://doi.org/10.1016/j.radmeas.2022.106828.

Ballarini, M., Wallinga, J., Murray, A.S., van Heteren, S., Oost, A.P., Bos, A.J.J., van Eijk, C.W.E., 2003. Optical dating of young coastal dunes on a decadal time scale. Quat. Sci. Rev. 22, 1011–1017. https://doi.org/10.1016/S0277-3791(03)00043-X. LED 2002.

Barnekow, L., Possnert, G., Sandgren, P., 1998. AMS 14C chronologies of Holocene lake sediments in the Abisko area, northern Sweden – a comparison between dated bulk sediment and macrofossil samples. GFF 120, 59–67. https://doi.org/10.1080/11035899801201059.

Barsanti, M., Garcia-Tenorio, R., Schirone, A., Rozmaric, M., Ruiz-Fernández, A.C., Sanchez-Cabeza, J.A., Delbono, I., Conte, F., De Oliveira Godoy, J.M., Heijnis, H., Eriksson, M., Hatje, V., Laissaoui, A., Nguyen, H.Q., Okuku, E., Al-Rousan, S.A., Uddin, S., Yii, M.W., Osvath, I., 2020. Challenges and limitations of the 210Pb sediment dating method: results from an IAEA modelling interlaboratory comparison exercise. Quat. Geochronol. 59. https://doi.org/10.1016/j.quageo.2020.101093.

Baskaran, M., 2012. Dating of biogenic and inorganic carbonates using 210Pb-226Ra disequilibrium method: a review. In: Baskaran, M. (Ed.), Handbook of Environmental Isotope Geochemistry, vol. I. Springer, Berlin, Heidelberg, pp. 789–809. https://doi.org/10.1007/978-3-642-10637-8_37.

Baskaran, M., Nix, J., Kuyper, C., Karunakara, N., 2014. Problems with the dating of sediment core using excess 210Pb in a freshwater system impacted by large scale watershed changes. J. Environ. Radioact. 138, 355–363. https://doi.org/10.1016/j.jenvrad.2014.07.006.

Bateman, M.D., Frederick, C.D., Jaiswal, M.K., Singhvi, A.K., 2003. Investigations into the potential effects of pedoturbation on luminescence dating. Quat. Sci. Rev., LED 22, 1169–1176. https://doi.org/10.1016/S0277-3791(03)00019-2, 2002.

Bateman, M.D., Boulter, C.H., Carr, A.S., Frederick, C.D., Peter, D., Wilder, M., 2007. Preserving the palaeoenvironmental record in Drylands: bioturbation and its significance for luminescence-derived chronologies. Sediment. Geol., Drylands 195, 5–19. https://doi.org/10.1016/j.sedgeo.2006.07.003.

Benninger, L.K., Aller, R.C., Cochran, J.K., Turekian, K.K., 1979. Effects of biological sediment mixing on the210Pb chronology and trace metal distribution in a Long Island Sound sediment core. Earth Planet Sci. Lett. 43, 241–259. https://doi.org/10.1016/0012-821X(79)90208-5.

Bertran, P., Andrieux, E., Leleu, S., Sicard-Delage, Z., Fores, B., Ouchaou, R., Weill, P., Reynaud, J.-Y., 2025. The Late Pleistocene – Holocene meandering lower Garonne River, southwest France: architecture of the valley fill and chronology, comparison with other European rivers. Geomorphology 468, 109469. https://doi.org/10.1016/j.geomorph.2024.109469.

Bevington, P.R., Robinson, D.K., 1994. Data Reduction and Error Analysis for the Physical Sciences, second ed. McGraw-Hill, New York NY.

Billy, J., Chaumillon, E., Féniès, H., Poirier, C., 2012. Tidal and fluvial controls on the morphological evolution of a lobate estuarine tidal bar: the Plassac Tidal Bar in the Gironde Estuary (France). Geomorphology 169–170, 86–97. https://doi.org/10.1016/j.geomorph.2012.04.015.

Bøtter-Jensen, L., Andersen, C.E., Duller, G.A.T., Murray, A.S., 2003. Developments in radiation, stimulation and observation facilities in luminescence measurements. Radiat. Meas., Proc. 10th Int. Conf. Luminesc. Electr.-Spin Resonan. Dat. (LED 2002) 37, 535–541. https://doi.org/10.1016/S1350-4487(03)00020-9.

Bouchet, V.M.P., Sauriau, P.-G., Debenay, J.-P., Mermillod-Blondin, F., Schmidt, S., Amiard, J.-C., Dupas, B., 2009. Influence of the mode of macrofauna-mediated bioturbation on the vertical distribution of living benthic foraminifera: first insight from axial tomodensitometry. J. Exp. Mar. Biol. Ecol. 371, 20–33. https://doi.org/10.1016/j.jembe.2008.12.012.

Bretel, P., Monfort, O., Froideval, L., Benoit, L., 2014. Mesure topographique par LiDAR aéroporté et Modèle Numérique Terrain de l'estuaire de l'Orne du 14/05/2014. SNO DYNALIT. https://doi.org/10.12770/86181d83-54c9-403d-af6c-3aeee9f73b6c.

Buylaert, J.P., Murray, A.S., Thomsen, K.J., Jain, M., 2009. Testing the potential of an elevated temperature IRSL signal from K-feldspar. In: Radiat. Meas., Proceedings of the 12th International Conference on Luminescence and Electron Spin Resonance Dating (LED 2008), vol 44, pp. 560–565. https://doi.org/10.1016/j.radmeas.2009.02.007.

Buylaert, J.-P., Thiel, C., Murray, A., Vandenberghe, D., Yi, S., Lu, H., 2011. IRSL and post-IR IRSL residual doses recorded in modern dust samples from the Chinese Loess Plateau. Geochronometria 38, 432–440. https://doi.org/10.2478/s13386-011-0047-0.

Cajthaml, J., 2011. Methods of Georeferencing Old Maps on the Example of Czech Early Maps.

Castaing, P., 1989. Co-oscillating tide controls long-term sedimentation in the Gironde Estuary, France. Mar. Geol. 89, 1–9. https://doi.org/10.1016/0025-3227(89)90024-8.

Chamberlain, E.L., Goodbred, S.L., Hale, R., Steckler, M.S., Wallinga, J., Wilson, C., 2020. Integrating geochronologic and instrumental approaches across the Bengal Basin. Earth Surf. Process. Landforms. 45, 56–74. https://doi.org/10.1002/esp.4687.

Chamberlain, E.L., Törnqvist, T., Shen, Z., Mauz, B., Wallinga, J., 2018. Anatomy of Mississippi Delta growth and its implications for coastal restoration. Sci. Adv. 4. https://doi.org/10.1126/sciadv.aar4740.

Chamberlain, E.L., Wallinga, J., 2019. Seeking enlightenment of fluvial sediment pathways by optically stimulated luminescence signal bleaching of river sediments and deltaic deposits. Earth Surf. Dyn. 7, 723–736. https://doi.org/10.5194/esurf-7-723-2019.

Chamberlain, E.L., Wallinga, J., Reimann, T., Goodbred, S.L., Steckler, M.S., Shen, Z., Sincavage, R., 2017. Luminescence dating of delta sediments: novel approaches explored for the Ganges-Brahmaputra-Meghna Delta. Quat. Geochronol. 41, 97–111. https://doi.org/10.1016/j.quageo.2017.06.006.

Chaumillon, E., Tessier, B., Reynaud, J.J.-Y., 2010. Stratigraphic records and variability of Incised valleys and estuaries along French coasts. Bull. Soc. Geol. Fr. 181, 75–85. https://doi.org/10.2113/gssgfbull.181.2.75.

Chaumillon, E., Féniès, H., Billy, J., Breilh, J., Richetti, H., 2013. Tidal and fluvial controls on the internal architecture and sedimentary facies of a lobate estuarine tidal bar (The Plassac Tidal Bar in the Gironde Estuary, France). Mar. Geol. 346. https://doi.org/10.1016/j.margeo.2013.07.017.

Colls, A.E., Stokes, S., Blum, M.D., Straffin, E., 2001. Age limits on the late quaternary evolution of the upper Loire River. Quat. Sci. Rev., TL/ESR Special 20, 743–750. https://doi.org/10.1016/S0277-3791(00)00048-2.

Colls, A.E.L., 1999. Optical Dating of Fluvial Sediments from the Loire Valley. France, Oxford.

Colman, S.M., Baucom, P.C., Bratton, J.F., Cronin, T.M., McGeehin, J.P., Willard, D., Zimmerman, A.R., Vogt, P.R., 2002. Radiocarbon dating, chronologic framework,

and changes in accumulation rates of Holocene estuarine sediments from Chesapeake Bay. Quat. Res. 57, 58–70. https://doi.org/10.1006/qres.2001.2285.
Culleton, B., Douglas, bullet, Kennett, J., Ingram, B., Erlandson, J., Erlandson, bullet J., Southon, 2006. Intrashell radiocarbon variability in marine mollusks. Radiocarbon 48, 387–400. https://doi.org/10.1017/S0033822200038820.
Cresswell, A.J., Carter, J., Sanderson, D.C.W., 2018. Dose rate conversion parameters: assessment of nuclear data. In: Radiat. Meas., 15th International Conference on Luminescence and Electron Spin Resonance Dating, 11-15 September 2017, vol 120, pp. 195–201. https://doi.org/10.1016/j.radmeas.2018.02.007.
Cunningham, A.C., Wallinga, J., 2010. Selection of integration time intervals for quartz OSL decay curves. Quat. Geochronol. 5, 657–666. https://doi.org/10.1016/j.quageo.2010.08.004.
Dallery, F., 1955. In: Picard, J., et al. (Eds.), Les rivages de la Somme, autrefois, aujourd'hui et demain, A.. Mémoires de la Société d'Emulation Historique et Littéraire d'Abbeville, Paris.
Das, O., Wang, Y., Donoghue, J., Xu, X., Coor, J., Elsner, J., Xu, Y., 2013. Reconstruction of paleostorms and paleoenvironment using geochemical proxies archived in the sediments of two coastal lakes in northwest Florida. Quat. Sci. Rev. 68, 142–153. https://doi.org/10.1016/j.quascirev.2013.02.014.
Deevey, E.S., Gross, M.S., Hutchinson, G.E., Kraybill, H.L., 1954. The natural c14 contents of materials from hard-water lakes. Proc. Natl. Acad. Sci. 40, 285–288. https://doi.org/10.1073/pnas.40.5.285.
Delsinne, N., 2005. Evolution pluri-millénaire à pluri-annuelle du prisme sédimentaire d'embouchure de la Seine : facteurs de contrôle naturels et d'origine anthropique (These de doctorat). Caen.
de Resseguier, A., 1983. A portable coring device for use in the intertidalenvironment. Mar. Geol. 52 (1–2), M19–M23. https://doi.org/10.1016/0025-3227(83)90015-4.
Dowey, P.J., Hodgson, D.M., Worden, R.H., 2012. Pre-requisites, processes, and prediction of chlorite grain coatings in petroleum reservoirs: a review of subsurface examples. Mar. Petrol. Geol. 32, 63–75. https://doi.org/10.1016/j.marpetgeo.2011.11.007.
Duller, G.a.T., 2008. Single-grain optical dating of Quaternary sediments: why aliquot size matters in luminescence dating. Boreas 37, 589–612. https://doi.org/10.1111/j.1502-3885.2008.00051.x.
Duller, G.A.T., 2003. Distinguishing quartz and feldspar in single grain luminescence measurements. Radiat. Meas. 37, 161–165. https://doi.org/10.1016/S1350-4487(02)00170-1.
Dumoulin, J.-P., Comby-Zerbino, C., Delque-Količ, E., Moreau, C., Caffy, I., Hain, S., Perron, M., Thellier, B., Setti, V., Berthier, B., Beck, L., 2017. Status report on sample preparation protocols developed at the LMC14 laboratory, Saclay, France: from sample collection to 14 C AMS measurement. Radiocarbon 59, 713–726. https://doi.org/10.1017/RDC.2016.116.
Durand, M., 2017. De l'estuaire à l'océan : expression des forçages locaux et globaux dans l'enregistrement sédimentaire de la dynamique de la Loire depuis l'Holocène Moyen.
Durand, M., Mojtahid, M., Maillet, G.M., Proust, J.-N., Lehay, D., Ehrhold, A., Barré, A., Howa, H., 2016. Mid- to late-Holocene environmental evolution of the Loire estuary as observed from sedimentary characteristics and benthic foraminiferal assemblages. J. Sea Res., Recent Past Sediment. Biogeochem. Benth. Ecosyst. Evol. Loire Est. (Western France) 118, 17–34. https://doi.org/10.1016/j.seares.2016.08.003.
Duteil, T., Bourillot, R., Braissant, O., Grégoire, B., Leloup, M., Portier, E., Brigaud, B., Féniès, H., Svahn, I., Henry, A., Yokoyama, Y., Visscher, P.T., 2022. Preservation of exopolymeric substances in estuarine sediments. Front. Microbiol. 13. https://doi.org/10.3389/fmicb.2022.921154.
Duteil, T., Bourillot, R., Gregoire, B., Virolle, M., Brigaud, B., Nouet, J., Braissant, O., Portier, E., Féniès, H., Patrier, P., Gontier, E., Svahn, I., Visscher, P., 2020. Experimental formation of clay-coated sand grains using diatom biofilm exopolymers. Geology 48 (1), 1012–1017. https://doi.org/10.1130/G47418.
England, J., Dyke, A., Coulthard, R., McNeely, R., Aitken, A., 2013. The exaggerated radiocarbon age of deposit-feeding molluscs in calcareous environments. Boreas 42, 362–373. https://doi.org/10.1111/j.1502-3885.2012.00256.x.
Erlandson, J., Moss, M., 1999. The systematic use of radiocarbon dating in Archaeological surveys in coastal and other erosional environments. Am. Antiq. 64, 431–443. https://doi.org/10.2307/2694143.
Figueres, G., Martin, J.M., Meybeck, M., Seyler, P., 1985. A comparative study of mercury contamination in the Tagus estuary (Portugal) and major French estuaries (Gironde, Loire, Rhône). Estuar. Coast Shelf Sci. 20, 183–203. https://doi.org/10.1016/0272-7714(85)90037-X.
Fenies, H., Tastet, J.-P., 1998. Facies and architecture of an estuarine tidal bar (the Trompeloup bar, Gironde Estuary, SW France). Mar. Geol. 150, 149–169. https://doi.org/10.1016/S0025-3227(98)00059-0.
Fitzsimmons, K., 2011. An assessment of the luminescence sensitivity of Australian quartz with respect to sediment history. Geochronometria 38, 199–208. https://doi.org/10.2478/s13386-011-0030-9.
Forman, S.L., Polyak, L., 1997. Radiocarbon content of pre-bomb marine mollusks and variations in the 14C Reservoir age for coastal areas of the Barents and Kara Seas, Russia. Geophys. Res. Lett. 24, 885–888. https://doi.org/10.1029/97GL00761.
Froidefond, J.M., Castaing, P., 1978. Analyse de l'évolution morphologique et estimation du volume des apports sédimentaires dans l'estuaire de la Gironde de 1825 à 1973.
Froideval, L., Monfort, C., Conessa, C., Benoit, L., 2017. Mesure topographique par LiDAR aéroporté et Modèle Numérique Terrain de l'estuaire de l'Orne du 09/05/2017. SNO DYNALIT. https://doi.org/10.12770/5d3e8de7-cff1-4e9c-87fe-66d1e3ca20c8.
Fruergaard, M., Andersen, T.J., Nielsen, L.H., Madsen, A.T., Johannessen, P.N., Murray, A.S., Kirkegaard, L., Pejrup, M., 2011. Punctuated sediment record resulting from channel migration in a shallow sand-dominated micro-tidal lagoon, Northern Wadden Sea, Denmark. Mar. Geol. 280 (1–4), 91–104. https://doi.org/10.1016/j.margeo.2010.12.003.
Fruergaard, M., Pejrup, M., Murray, A.S., Andersen, T.J., 2015. On luminescence bleaching of tidal channel sediments. Geogr. Tidsskr.-Dan. J. Geogr. 115, 57–65. https://doi.org/10.1080/00167223.2015.1011418.
Fruergaard, M., Tessier, B., Poirier, C., Mouazé, D., Weill, P., Noël, S., 2020. Depositional controls on a hypertidal barrier-spit system architecture and evolution, Pointe du Banc spit, north-western France. Sedimentology 67 (1), 502–533. https://doi.org/10.1111/sed.12652.
Galbraith, R.F., 2005. Statistics for Fission Track Analysis. Chapman and Hall/CRC, New York. https://doi.org/10.1201/9781420034929.
Gao, S., Collins, M.B., 2014. Holocene sedimentary systems on continental shelves. Mar. Geol. 352, 268–294. https://doi.org/10.1016/j.margeo.2014.03.021, 50th Anniversary Special Issue.
Gao, L., Long, H., Shen, J., Yu, G., Liao, M., Yin, Y., 2017. Optical dating of Holocene tidal deposits from the southwestern coast of the South Yellow Sea using different grain-size quartz fractions. J. Asian Earth Sci. 135, 155–165. https://doi.org/10.1016/j.jseaes.2016.12.036.
Godwin, H., 1951. Comments on radiocarbon dating for samples from the British Isles. Am. J. Sci. 249, 301–307. https://doi.org/10.2475/ajs.249.4.301.
Gómez, E.A., Borel, C.M., Aguirre, M.L., Martínez, D.E., 2008. Radiocarbon reservoir ages and hardwater effect for the northeastern coastal waters of Argentina. Radiocarbon 50, 119–129. https://doi.org/10.1017/S003382220004340X.
Goslar, T., Czernik, J., Goslar, E., 2004. Low-energy 14C AMS in Poznań radiocarbon Laboratory, Poland. Proceedings of the Ninth International Conference on Accelerator Mass Spectrometry 223–224. Nucl. Instrum. Methods Phys. Res. Sect. B Beam Interact. Mater. At., pp. 5–11. https://doi.org/10.1016/j.nimb.2004.04.005
GRESARC, 2003. Etude d'impact du prélèvement des matériaux et de leur refoulement depuis le canal maritime - Partie 1 : Etat Initial, Groupe de Recherche sur les Environnements Sédimentaires Aménagés et les Risques Côtiers, Société des Matériaux Caennais (Rapport technique).
Griffiths, J., Worden, R.H., Utley, J.E.P., Brostrøm, C., Martinius, A.W., Lawan, A.Y., Al-Hajri, A.I., 2021. Origin and distribution of grain-coating and pore-filling chlorite in deltaic sandstones for reservoir quality assessment. Mar. Petrol. Geol. 134, 105326. https://doi.org/10.1016/j.marpetgeo.2021.105326.
Grimm, B.L., Spero, H.J., Harding, J.M., Guilderson, T.P., 2017. Seasonal radiocarbon reservoir ages for the 17th century James River, Virginia estuary. Quat. Geochronol. 41, 119–133. https://doi.org/10.1016/j.quageo.2017.03.002.
Guérin, G., Christophe, C., Philippe, A., Murray, A.S., Thomsen, K.J., Tribolo, C., Urbanova, P., Jain, M., Guibert, P., Mercier, N., Kreutzer, S., Lahaye, C., 2017. Absorbed dose, equivalent dose, measured dose rates, and implications for OSL age estimates: introducing the Average Dose Model. Quat. Geochronol. 41, 163–173. https://doi.org/10.1016/j.quageo.2017.04.002.
Hansen, V., Murray, A., Buylaert, J.-P., Yeo, E.-Y., Thomsen, K., 2015. A new irradiated quartz for beta source calibration. In: Radiation Measurements, 14th International Conference on Luminescence and Electron Spin Resonance Dating, 7–11 July, 2014, Montréal, Canada, vol 81, pp. 123–127. https://doi.org/10.1016/j.radmeas.2015.02.017.
Hansen, V., Murray, A., Thomsen, K., Jain, M., Autzen, M., Buylaert, J.-P., 2018. Towards the origins of over-dispersion in beta source calibration. In: Radiat. Meas., 15th International Conference on Luminescence and Electron Spin Resonance Dating, 11-15 September 2017, vol 120, pp. 157–162. https://doi.org/10.1016/j.radmeas.2018.05.014.
Heaton, T.J., Köhler, P., Butzin, M., Bard, E., Reimer, R.W., Austin, W.E.N., Ramsey, C.B., Grootes, P.M., Hughen, K.A., Kromer, B., Reimer, P.J., Adkins, J., Burke, A., Cook, M. S., Olsen, J., Skinner, L.C., 2020. Marine20—the marine radiocarbon age calibration curve (0–55,000 cal BP). Radiocarbon 62, 779–820. https://doi.org/10.1017/RDC.2020.68.
Hofmann, C., Tesson, S., 2012. Artistes de la carte: De la Renaissance au XXIe siècle, l'explorateur, le stratège, le géographe. AUTREMENT, Paris.
Hogg, A.G., Higham, T.F.G., Dahm, J., 1997. 14C dating of modern marine and estuarine Shellfish. Radiocarbon 40, 975–984. https://doi.org/10.1017/S0033822200018944.
Holmquist, J.R., Reynolds, L., Brown, L.N., Southon, J.R., Simms, A.R., MacDonald, G. M., 2015. Marine radiocarbon reservoir values in Southern California Estuaries: interspecies, latitudinal, and interannual variability. Radiocarbon 57 (3), 449–458. https://doi.org/10.2458/azu_rc.57.18389.
Hughes, R.N., 1969. A study of feeding in Scrobicularia plana. J. Mar. Biol. Assoc. U. K. 49, 805–823. https://doi.org/10.1017/S0025315400037309.
Huntley, D.J., Baril, M., 1997. The K content of the K-feldspars being measured in optical dating or in thermoluminescence dating. Anc. Tl 15, 11–13.
Huntley, D.J., Clague, J.J., 1996. Optical dating of Tsunami-Laid sands. Quat. Res. 46, 127–140. https://doi.org/10.1006/qres.1996.0053.
Hydroportail, 2023. Données hydrologiques de synthèse [WWW Document]. URL. https://www.hydro.eaufrance.fr/.
Ingram, B., Southon, J., 1996. Reservoir ages in eastern Pacific coastal and estuarine waters. Radiocarbon 38. https://doi.org/10.1017/S0033822200030101.
Jain, M., Murray, A., Botter-Jensen, L., 2004. Optically stimulated luminescence dating: how significant is incomplete light exposure in fluvial environments? Quaternaire 15, 143–157. https://doi.org/10.3406/quate.2004.1762.
Jalón-Rojas, I., Schmidt, S., Sottolichio, A., 2015. Turbidity in the fluvial Gironde Estuary (southwest France) based on 10-year continuous monitoring: sensitivity to hydrological conditions. Hydrol. Earth Syst. Sci. 19, 2805–2819. https://doi.org/10.5194/hess-19-2805-2015.

Jankowski, N., Jacobs, Z., Goldberg, P., 2015. Optical dating and soil micromorphology at MacCauley's beach, New South Wales, Australia. Earth Surf. Process. Landf. 40. https://doi.org/10.1002/esp.3622.
Kim, J.C., Cheong, D., Shin, S., Park, Y.-H., Hong, S.S., 2015. OSL chronology and accumulation rate of the Nakdong deltaic sediments, southeastern Korean Peninsula. Quat. Geochronol., LED14 Proc. 30, 245–250. https://doi.org/10.1016/j.quageo.2015.01.006.
Kitis, G., Polymeris, G.S., Peng, J., 2025. Determining equivalent dose for optically stimulated luminescence (OSL) dating with physically meaningful dose response curves. Quat. Geochronol. 88, 101671. https://doi.org/10.1016/j.quageo.2025.101671.
Latapy, A., 2020. Influence des modifications morphologiques de l'avant-côte sur l'hydrodynamisme et l'évolution du littoral des Hauts-de-France depuis le XIXe siècle (phdthesis). Université du Littoral Côte d'Opale.
Lescure, S., 2015. La Garonne maritime à l'holocène : dynamique, environnements et occupation humaine (phdthesis). Université Panthéon-Sorbonne - Paris I.
Loquet, N., Rybarczyk, H., Elkaim, B., 2000. Échanges de sels nutritifs entre la zone côtière et un système estuarien intertidal : la baie de Somme (Manche, France). Oceanol. Acta 23, 47–64. https://doi.org/10.1016/S0399-1784(00)00117-1.
Lougheed, B.C., Filipsson, H.L., Snowball, I., 2013. Large spatial variations in coastal 14C reservoir age – a case study from the Baltic Sea. Clim. Past 9, 1015–1028. https://doi.org/10.5194/cp-9-1015-2013.
Lougheed, B.C., Obrochta, S.P., Lenz, C., Mellström, A., Metcalfe, B., Muscheler, R., Reinholdsson, M., Snowball, I., Zillén, L., 2017. Bulk sediment 14C dating in an estuarine environment: how accurate can it be? Paleoceanography 32, 123–131. https://doi.org/10.1002/2016PA002960.
Lougheed, B.C., van der Lubbe, H.J.L., Davies, G.R., 2016. 87Sr/86Sr as a quantitative geochemical proxy for 14C reservoir age in dynamic, brackish waters: assessing applicability and quantifying uncertainties. Geophys. Res. Lett. 43, 735–742. https://doi.org/10.1002/2015GL066983.
Madsen, A., Buylaert, J.-P., Murray, A., 2011a. Luminescence dating of young coastal deposits from New Zealand using feldspar. Geochronometria 38, 379–390. https://doi.org/10.2478/s13386-011-0042-5.
Madsen, A., Murray, A.S., Jain, M., Andersen, T.J., Pejrup, M., 2011b. A new method for measuring bioturbation rates in sandy tidal flat sediments based on luminescence dating. Estuar. Coast Shelf Sci. 92, 464–471. https://doi.org/10.1016/j.ecss.2011.02.004.
Madsen, A.T., Murray, A.S., 2009. Optically stimulated luminescence dating of young sediments: a review. Geomorphol. Luminesc. Dat. Geomorphol. 109, 3–16. https://doi.org/10.1016/j.geomorph.2008.08.020.
Madsen, A.T., Murray, A.S., Andersen, T.J., Pejrup, M., 2007a. Optical dating of young tidal sediments in the Danish Wadden Sea. Quat. Geochronol. 2, 89–94. https://doi.org/10.1016/j.quageo.2006.05.008. LED 2005.
Madsen, A.T., Murray, A.S., Andersen, T.J., Pejrup, M., 2007b. Temporal changes of accretion rates on an estuarine salt marsh during the late Holocene — reflection of local sea level changes? The Wadden Sea, Denmark. Mar. Geol. 242, 221–233. https://doi.org/10.1016/j.margeo.2007.03.001.
Madsen, A.T., Murray, A.S., Andersen, T.J., 2007c. Optical dating of dune ridges on Rømø: a barrier Island in the Wadden sea, Denmark. J. Coast Res. 23, 1259–1269. https://doi.org/10.2112/05-0471.1.
Madsen, A.T., Murray, A.S., Andersen, T.J., Pejrup, M., Breuning-Madsen, H., 2005. Optically stimulated luminescence dating of young estuarine sediments: a comparison with 210Pb and 137Cs dating. Mar. Geol. 214, 251–268. https://doi.org/10.1016/j.margeo.2004.10.034.
Mangerud, J., Bondevik, S., Gulliksen, S., Karin Hufthammer, A., Høisæter, T., 2006. Marine 14C reservoir ages for 19th century whales and molluscs from the North Atlantic. Quat. Sci. Rev., Crit. Quatern. Stratigr. 25, 3228–3245. https://doi.org/10.1016/j.quascirev.2006.03.010.
Mauz, B., Baeteman, C., Bungenstock, F., Plater, A.J., 2010. Optical dating of tidal sediments: Potentials and limits inferred from the North Sea coast. Quat. Geochronol. 5, 667–678. https://doi.org/10.1016/j.quageo.2010.05.004.
Medialdea, A., Thomsen, K.J., Murray, A., Benito, G., 2014. Reliability of equivalent-dose determination and age-models in the OSL dating of historical and modern palaeoflood sediments. Quat. Geochronol. 22, 11–24. https://doi.org/10.1016/j.quageo.2014.01.004.
Migniot, C., 1971. L'évolution de la Gironde au cours des temps (No. Bul. Inst. Geol. Bas. Aquitaine. Bordeaux).
Miguel, S., Bolívar, J.P., García-Tenorio, R., 2003. Mixing, sediment accumulation and focusing using 210Pb and 137Cs. J. Paleolimnol. 29, 1–11. https://doi.org/10.1023/A:1022864615111.
Moreau, C., Caffy, I., Comby, C., Delqué-Kolic, E., Dumoulin, J.-P., Hain, S., Quiles, A., Setti, V., Souprayen, C., Thellier, B., Vincent, J., 2013. Research and development of the artemis 14C AMS facility: status report. Radiocarbon 55, 331–337. https://doi.org/10.1017/S0033822200057441.
Murray, A., Arnold, L.J., Buylaert, J.-P., Guérin, G., Qin, J., Singhvi, A.K., Smedley, R., Thomsen, K.J., 2021. Optically stimulated luminescence dating using quartz. Nat. Rev. Methods Primers 1, 1–31. https://doi.org/10.1038/s43586-021-00068-5.
Murray, A.S., Buylaert, J.P., Thomsen, K.J., Jain, M., 2009. The effect of preheating on the IRSL signal from feldspar. In: Radiat. Meas., Proceedings of the 12th International Conference on Luminescence and Electron Spin Resonance Dating (LED 2008), vol 44, pp. 554–559. https://doi.org/10.1016/j.radmeas.2009.02.004.
Murray, A.S., Helsted, L.M., Autzen, M., Jain, M., Buylaert, J.P., 2018. Measurement of natural radioactivity: calibration and performance of a high-resolution gamma spectrometry facility. In: Radiat. Meas., 15th International Conference on Luminescence and Electron Spin Resonance Dating, 11-15 September 2017, vol 120, pp. 215–220. https://doi.org/10.1016/j.radmeas.2018.04.006.
Murray, A.S., Marten, R., Johnston, A., Martin, P., 1987. Analysis for naturally occurring radionuclides at environmental concentrations by gamma spectrometry. J. Radioanal. Nucl. Chem. 115, 263–288. https://doi.org/10.1007/BF02037443.
Murray, A., Olley, J., 2002. Precision and accuracy in the optically stimulated luminescence dating of sedimentary quartz: a status review. Geochronometria 21, 1–16.
Murray, A.S., Thomsen, K.J., Masuda, N., Buylaert, J.P., Jain, M., 2012. Identifying well-bleached quartz using the different bleaching rates of quartz and feldspar luminescence signals. In: Radiat. Meas., Proceedings of the 13th International Conference on Luminescence and Electron Spin Resonance Dating, 10–14 July, 2011, Toruń, Poland, vol 47, pp. 688–695. https://doi.org/10.1016/j.radmeas.2012.05.006.
Murray, A., Wintle, A.G., 2000. Luminescence dating of quartz using an improved single-aliquot regenerative-dose protocol. Radiat. Meas. 32, 57–73. https://doi.org/10.1016/S1350-4487(99)00253-X.
Murray, A.S., Wintle, A.G., 2003. The single aliquot regenerative dose protocol: potential for improvements in reliability. In: Radiation Measurements, Proceedings of the 10th international Conference on Luminescence and Electron-Spin Resonance Dating (LED 2002), vol 37, pp. 377–381. https://doi.org/10.1016/S1350-4487(03)00053-2.
Nasseh, A., Texier, H., Lacroix, M., Ouddane, B., 1999. Transport de la charge solide dans le bassin versant de l'Orne.Composition, variabilité et flux. Hydroécol. Appliquée 11, 1994–1995. https://doi.org/10.1051/hydro:1999004.
Nian, X., Zhang, W., Wang, Z., Sun, Q., Chen, J., Chen, Z., Hutchinson, S.M., 2018a. The chronology of a sediment core from incised valley of the Yangtze River delta: comparative OSL and AMS 14C dating. Mar. Geol. 395, 320–330. https://doi.org/10.1016/j.margeo.2017.11.008.
Nian, X., Zhang, W., Wang, Z., Sun, Q., Chen 陈 静, J., Chen, Z., 2018b. Optical dating of Holocene sediments from the Yangtze river (Changjiang) delta, China. Quat. Int. 467. https://doi.org/10.1016/j.quaint.2018.01.011.
Niu, W., Nian, X., Zhao, L., Zhai, Y., Meadows, M.E., Zhang, W., Wang, Z., 2022. Luminescence characteristics of muddy sediments in the turbidity maximum zone of the Yangtze River mouth and implications for the depositional mechanisms. Front. Earth Sci. 10. https://doi.org/10.3389/feart.2022.972642.
Olley, J.M., Pietsch, T., Roberts, R.G., 2004. Optical dating of Holocene sediments from a variety of geomorphic settings using single grains of quartz. Geomorphology 60, 337–358. https://doi.org/10.1016/j.geomorph.2003.09.020.
Olsen, J., Ascough, P., Lougheed, B.C., Rasmussen, P., 2017. Radiocarbon dating in estuarine environments. In: Weckström, K., Saunders, K.M., Gell, P.A., Skilbeck, C.G. (Eds.), Applications of Paleoenvironmental Techniques in Estuarine Studies. Springer, Netherlands, Dordrecht, pp. 141–170. https://doi.org/10.1007/978-94-024-0990-1_7.
Pannozzo, N., Smedley, R.K., Chiverrell, R.C., Carnacina, I., Leonardi, N., 2022. An integration of Numerical modeling and paleoenvironmental analysis reveals the effects of Embankment construction on long-term salt marsh accretion. J. Geophys. Res. Earth Surf. 127. https://doi.org/10.1029/2021JF006524 e2021JF006524.
Paradis, D., Pasquet, A., Dalphinet, A., Kpogo-Nuwoklo, K., Michaud, H., Baraille, R., Jourdan, D., Ohl, P., Le Belleguic, R., Ayache, D., Bataille, C., Ciavaldini, M., Brosse, F., Krien, Y., 2024. Le projet HOMONIM, en soutien des prévisions d'inondation côtière. LHB 110, 2332256. https://doi.org/10.1080/27678490.2024.2332256.
Pellerin Le Bas, X., 2018. Morphodynamique des deltas de jusant et des flèches sableuses en domaine macrotidal : les embouchures de l'Orne et de la Dives. These de doctorat), Normandie.
Perilla-Castillo, P.J., Driese, S.G., Horn, S.P., Rittenour, T.M., Nelson, M.S., McKay, L.D., 2023. Using soil micromorphology to assess the reliability of radiocarbon and OSL dating of fluvial deposits. Phys. Geogr. 44, 710–762. https://doi.org/10.1080/02723646.2023.2178691.
Philippsen, B., Heinemeier, J., 2013. Freshwater reservoir effect variability in northern Germany. Radiocarbon 55, 1085–1101. https://doi.org/10.1017/S0033822200048001.
Pietsch, T.J., 2009. Optically stimulated luminescence dating of young (<500 years old) sediments: testing estimates of burial dose. Quat. Geochronol., Dat. Rec. Past 4, 406–422. https://doi.org/10.1016/j.quageo.2009.05.013.
Pietsch, T.J., Olley, J.M., Nanson, G.C., 2008. Fluvial transport as a natural luminescence sensitiser of quartz. Quat. Geochronol. 3, 365–376. https://doi.org/10.1016/j.quageo.2007.12.005.
Prescott, J.R., Hutton, J.T., 1994. Cosmic ray contributions to dose rates for luminescence and ESR dating: large depths and long-term time variations. Radiat. Meas. 23, 497–500. https://doi.org/10.1016/1350-4487(94)90086-8.
Qiaola, S., Nguyen, T.M.L., Ta, T.K.O., Nguyen, V.L., Gugliotta, M., Saito, Y., Kitagawa, H., Nakashima, R., Tamura, T., 2022. Luminescence dating of Holocene sediment cores from a wave-dominated and mountainous river delta in central Vietnam. Quat. Geochronol. 70, 101277. https://doi.org/10.1016/j.quageo.2022.101277.
Ramsey, C., 2009. Bayesian analysis of radiocarbon dates. Radiocarbon 51, 337–360. https://doi.org/10.2458/azu_js_rc.51.3494.
Ramsey, C.B., 1995. Radiocarbon calibration and analysis of stratigraphy: the OxCal program. Radiocarbon 37, 425–430. https://doi.org/10.1017/S0033822200030903.
Reimann, T., Tsukamoto, S., 2012. Dating the recent past (<500 years) by post-IR IRSL feldspar – examples from the north sea and baltic sea coast. In: Quat. Geochronol., 13th International Conference on Luminescence and Electron Spin Resonance Dating - LED 2011 Dedicated to J. Prescott and G. Berger, vol 10, pp. 180–187. https://doi.org/10.1016/j.quageo.2012.04.011.

Reimer, P.J., Reimer, R.W., 2001. A marine reservoir correction database and on-line interface. Radiocarbon 43, 461–463. https://doi.org/10.1017/S0033822200038339.

Ritchie, J.C., McHenry, J.R., 1990. Application of radioactive fallout cesium-137 for measuring soil erosion and sediment accumulation rates and patterns: a review. J. Environ. Qual. 19, 215–233. https://doi.org/10.2134/jeq1990.00472425001900020006x.

Russell, N., 2011. Marine Radiocarbon Reservoir Effects (MRE) in Archaeology: Temporal and Spatial Changes through the Holocene within the UK Coastal Environment. University of Glasgow (PhD).

Sabatier, P., Dezileau, L., Blanchemanche, P., Siani, G., Condomines, M., Bentaleb, I., Piquès, G., 2010. Holocene variations of radiocarbon reservoir ages in a Mediterranean Lagoonal system. Radiocarbon 52, 91–102. https://doi.org/10.1017/S0033822200045057.

Sambridge, M., Braun, J., McQueen, H., 1995. Geophysical parametrization and interpolation of irregular data using natural neighbours. Geophys. J. Int. 122, 837–857. https://doi.org/10.1111/j.1365-246X.1995.tb06841.x.

Schäfer, J., Blanc, G., Lapaquellerie, Y., Maillet, N., Maneux, E., Etcheber, H., 2002. Ten-year observation of the Gironde tributary fluvial system: fluxes of suspended matter, particulate organic carbon and cadmium. Mar. Chem., 6th Int. Symp. Model Estuar. 79, 229–242. https://doi.org/10.1016/S0304-4203(02)00066-X.

Shom-Service Hydrographique Et Océanographique De La Marine, 2022. Données du réseau de référence des observations marégraphiques (REFMAR). https://services.data.shom.fr:/geonetwork/system/api/records/MAREE_COURANTS_RAM_PACK.xml.

Singarayer, J.S., Bailey, R.M., Ward, S., Stokes, S., 2005. Assessing the completeness of optical resetting of quartz OSL in the natural environment. Radiat. Meas. 40, 13–25. https://doi.org/10.1016/j.radmeas.2005.02.005.

Soares, C., Sobral, P., 2009. Bioturbation and Erodibility of sediments from the Tagus estuary. J. Coast Res. 1429–1433.

Sohbati, R., Kook, M., Pirtzel, L., Thomsen, K., 2021. Safelight for OSL Dating Laboratories: a Follow-Up Study, vol. 39, p. 2021.

Stokes, S., Bray, H.E., Blum, M.D., 2001. Optical resetting in large drainage basins: tests of zeroing assumptions using single-aliquot procedures. Quat. Sci. Rev., TL/ESR Special 20, 879–885. https://doi.org/10.1016/S0277-3791(00)00045-7.

Straffin, E., Blum, M., 2001. Fluvial responses to external forcing. https://doi.org/10.1201/9781439824672.ch6.

Straffin, E., Blum, M., Colls, A., Stokes, S., 1999. Alluvial stratigraphy of the Loire and Arroux rivers (Burgundy, France). Quaternaire 10, 271–282. https://doi.org/10.3406/quate.1999.1648.

Stuiver, M., Braziunas, T.F., 1993. Modeling atmospheric 14C influences and 14C ages of marine samples to 10,000 BC. Radiocarbon 35, 137–189. https://doi.org/10.1017/S0033822200013874.

Stuiver, M., Pearson, G.W., Braziunas, T., 1986. Radiocarbon age calibration of marine samples back to 9000 cal Yr BP. Radiocarbon 28, 980–1021. https://doi.org/10.1017/S0033822200060264.

Stuiver, M., Polach, H., 2006. Reporting of C-14 data—discussion. Radiocarbon 19. https://doi.org/10.2458/azu_js_rc.v.493.

Swarzenski, P.W., 2013. 210Pb dating. In: Rink, W.J., Thompson, J. (Eds.), Encyclopedia of Scientific Dating Methods. Springer, Netherlands, Dordrecht, pp. 1–11. https://doi.org/10.1007/978-94-007-6326-5_236-1.

SYstème de Veille dans l'Estuaire de la Loire (SYVEL), 2023. Bulletin SYVEL n°11. Groupement d'Intérêt Public Loire Estuaire. https://www.loire-estuaire.org.

Tessier, B., 1993. Upper intertidal rhythmites in the Mont-Saint-Michel Bay (NW France): perspectives for paleoreconstruction. Mar.Geol. 110 (3–4), 355–367.

Tessier, B., 2023. Tidal rhythmites: their contribution to the characterization of tidal dynamics and environments. In: Green, M., Duarte, J.C. (Eds.), A Journey through Tides. Elsevier, pp. 283–305. https://doi.org/10.1016/B978-0-323-90851-1.00015-7.

Thiel, C., Buylaert, J.-P., Murray, A., Terhorst, B., Hofer, I., Tsukamoto, S., Frechen, M., 2011. Luminescence dating of the Stratzing loess profile (Austria) – testing the potential of an elevated temperature post-IR IRSL protocol. Quatern. Int., Loess in Eurasia 234, 23–31. https://doi.org/10.1016/j.quaint.2010.05.018.

Tisnérat-Laborde, N., Paterne, M., Métivier, B., Arnold, M., Yiou, P., Raynaud, S., 2010. Variability of the northeast Atlantic sea surface Δ14C and marine reservoir age and the North Atlantic Oscillation (NAO). Quat. Sci. Rev. 29, 2633–2646. https://doi.org/10.1016/j.quascirev.2010.06.013.

Tukey, J.W., 1977. Exploratory Data Analysis. Addison Wesley, Reading, Mass.

Turki, I., Le Bot, S., Lecoq, N., Shafiei, H., Michel, C., Deloffre, J., Héquette, A., Sipka, V., Lafite, R., 2021. Morphodynamics of intertidal dune field in a mixed wave-tide environment: Case of Baie de Somme in Eastern English Channel. Mar. Geol. 431, 106381. https://doi.org/10.1016/j.margeo.2020.106381.

Ulm, S., 2002. Marine and estuarine reservoir effects in central Queensland, Australia: determination of ΔR values. Geoarchaeology 17, 319–348. https://doi.org/10.1002/gea.10017.

Vartanian, E., Soler, L., Roque, C., Dupont, C., Save, S., 2013. Chronologie par C14 et détermination des effets réservoir selon les différentes espèces de coquillages. Le cas du site des quatre Chevaliers à Périgny (Charente-Maritime) et application à la correction de l'âge d'un ossement humain.

Virolle, M., 2019. Origine et prédiction spatio-temporelle des tapissages argileux dans les réservoirs silicoclastiques - Apports de la comparaison entre des réservoirs enfouis (Permien et Crétacé) et un analogue actuel (estuaire de la Gironde).

Virolle, M., Brigaud, B., Bourillot, R., Féniès, H., Portier, E., Duteil, T., Nouet, J., Patrier, P., Beaufort, D., 2019a. Detrital clay grain coats in estuarine clastic deposits: origin and spatial distribution within a modern sedimentary system, the Gironde Estuary (south-west France). Sedimentology 66, 859–894. https://doi.org/10.1111/sed.12520.

Virolle, M., Brigaud, B., Luby, S., Portier, E., Féniès, H., Bourillot, R., Patrier, P., Beaufort, D., 2019b. Influence of sedimentation and detrital clay grain coats on chloritized sandstone reservoir qualities: insights from comparisons between ancient tidal heterolithic sandstones and a modern estuarine system. Mar. Petrol. Geol. 107, 163–184. https://doi.org/10.1016/j.marpetgeo.2019.05.010.

Virolle, M., Féniès, H., Brigaud, B., Bourillot, R., Portier, E., Patrier, P., et al., 2020. Facies associations, detrital clay grain coats and mineralogical characterization of the Gironde estuary tidal bars: a modern analogue for deeply buried estuarine sandstone reservoirs. Mar. Petrol. Geol. 114, 104225.

Wallinga, J., 2002. Detection of OSL age overestimation using single–aliquot techniques. Geochronometria 21.

Wang, Y., Long, H., Yi, L., Yang, L., Ye, X., Shen, J., 2015. OSL chronology of a sedimentary sequence from the inner-shelf of the East China Sea and its implication on post-glacial deposition history. Quat. Geochronol., LED14 Proc. 30, 282–287. https://doi.org/10.1016/j.quageo.2015.06.005.

Wooldridge, L., Worden, R., Griffiths, J., Utley, J., 2017. Clay-coated sand grains in petroleum reservoirs: understanding their distribution via A modern analogue. J. Sediment. Res. 87, 338–352. https://doi.org/10.2110/jsr.2017.20.

Wright, D.K., 2017. Accuracy vs. Precision: understanding potential errors from radiocarbon dating on African Landscapes. Afr. Archaeol. Rev. 34, 303–319. https://doi.org/10.1007/s10437-017-9257-z.

Yi, L., Ye, X., Chen, J., Li, Y., Long, H., Wang, X., Du, J., Zhao, S., Deng, C., 2014. Magnetostratigraphy and luminescence dating on a sedimentary sequence from northern East China Sea: constraints on evolutionary history of eastern marginal seas of China since the Early Pleistocene. Quat. Int. 349, 316–326. https://doi.org/10.1016/j.quaint.2014.07.038.